

26th june 2020

1 Response letter

2

3 We highly value the comments and suggestions of Reviewers and we have improved the
4 manuscript accordingly. We hope you find the answers and the revised version appropriate.
5 Here below are our answers to the comments and manuscript with changes

6

7

8

9 **Associate Editor Decision: Publish subject to minor revisions (review by editor)** (04 Jun
10 2020) by Michael Bahn

11 Comments to the Author:

12 Dear authors,

13

14 both reviewers think that their concerns have been largely addressed, even though some of their
15 suggestions for additional relevant testing were not taken up by you. The reviewers have
16 provided a number of excellent specific suggestions for further improvement, which I kindly ask
17 you to consider during this next round of revisions. Please include also a more critical
18 assessment of the limitations of the current model version.

19

20 Best regards,

21

22 Michael Bahn

23

24 *-We have now added a critical assessment of the limitations of the current model version to the
25 end of the discussion*

26

27 Referee 1

This is my second review of this manuscript for Biogeosciences and I am pleased that the authors incorporated many of the suggestions made by me and the other reviewer. In brief, the strength of the study emerges from their combining an individual-based, two species competition model of Sphagnum community interactions with underlying functional models of water and carbon dynamics and linking it to a hydrology simulation model. Historically, most modeling efforts have focused on understanding and modeling the mechanisms of competition and function in Sphagnum. One of the highlights of this study is the connection to an existing hydrology and surface exchange model that was used to generate local environmental conditions that served as forcing variables for the simulation. Overall, I believe that this manuscript represents a valuable step in developing predictive models of peatland function.

I still have a couple of issues that I think the authors ought to address and then provide a list of minor edits.

A. There are still many places where “water retention” and “water content” are used

synonymously. In my mind, retention is when existing water is not released via evaporation or drainage. I don't think this is the meaning the authors intend. Most of the times, I think the authors mean capitulum "water content". This incorporates fluxes in and out, but also the capacity for storage. I think the language needs to be clarified and it begins with its usage in the title. Here is a list of places that I found places where this should be clarified: L2, L28, L35, L75, and L522; there may be others.

-Changed as suggested.

B. I remain surprised that the authors still did not show sample light response curves in the Appendix, which were the source of many of their photosynthetic parameters; both reviewers questioned their measurements, especially with regards to the long time for samples to desiccate within the chamber. In the appendix, data for the photosynthetic—water content relationships are shown (Fig B2). I think light response curves should be added. They may be very useful if this study is used for comparative purposes in the future.

-The measured light response curves for S. magellanicum and S. fallax are now added to Appendix B as Figure B1.

Minor edits

C. L15: what do you mean by "dynamic community structure"? There should be a better way to state this.

-Clarified in lines 15-19 to "Current peatland models generally treat vegetation as a static community, although plant community structure is known to alter as a response to environmental change. Because vegetation structure and ecosystem functioning are tightly linked, realistic projections of peatland response to climate change requires including vegetation dynamics in ecosystem models."

D. L25. The description of what PMS does should be more clear. Perhaps it would be better worded by placing competition up front. "PMS employs a, stochastic, individual-based approach to simulating competition based on species' differences in functional traits."

Changed in lines 25-30 into: In this study, we developed the Peatland Moss Simulator (PMS), simulating community dynamics of the peatland moss layer. PMS is a process-based model that employs a stochastic, individual-based approach simulating competition within peatland moss layer based on species differences in functional traits.

E. L35: replace "retention" with "relations"

-changed

F. L53: unclear what "dynamic community structure" relates to. "lack mechanisms that underlie and cause dynamic community processes"?

-Clarified. Now says "Peatland models have generally considered vegetation structure unrealistically as static component"

G. L55: delete "in order"

-deleted

H. L55: delete after “and the research community”
-deleted

I. L73: replace “the peers” with “its peers”.
-changed

J. L75: and water storage
-added

K. L87: I think the ability to carry out such a quantitative study is not new and don’t believe this has been a great hindrance.
-deleted

L. L93: occur to occurs
-changed

M. L98: rely to relies
-changed

N. L114: replace “locates” to “is located”-*changed*
O. L118: to “10% of the surface is occupied....”
-changed

P. L128: to “flow with...”
-changed

Q. L143: “race for space” to competition
-changed

R. L414: change PCS to PMS
-changed

S. L491: lawnss to lawns
-changed

T. L535: delete the
-deleted

U. L573 and 577: replace dynamical with dynamic
-changed

28

29 Referee 2

30

Dear authors,

Thank you for addressing the concerns raised by me and the other reviewer. Several points have now been clarified in the text (please do check the grammar, which is not flawless in the added sections). There are a few remarks that you have responded to only in your reply to us but not in the main text (e.g. my previous points 3b (horizontal water exchange), point C and D of reviewer 3 (autogenic processes leading to hummock formation and differences in moss hydraulic conductivity)). I think those are missed chances of improving the outlook section for your model. In general, I would appreciate a more explicit acknowledgment of the limitations of your model. After all, even if you managed to recreate some 'realistic' patterns, several potentially important processes are still missing from the model, so you cannot be sure whether you produced these patterns for the right reasons. It is absolutely fine to start with a simple model (even if your main purpose is to 'illustrate the reality' L188 in your response) and to 'leave perfection for later' (L70 in your response), but thereby it is helpful to line out the path to perfection (well, at least to a model in which the importance of additional processes has been tested) for the readers.

-We have now included a section in the discussion that focus on the limitation of our model, in lines 588-617. We had that in the first version of the manuscript but it was accidentally left out when we combined the two manuscripts (empirical and modelling) into one and tried to make it concise.

Also, I think there are two points (6 and 7) that I think you may have misunderstood, so that I will try to formulate them better here. I pasted my old remark and your reply in here to keep track of the context.

My previous point 6 and your reply:

As an important difference between your and previous models lies in the coupling to environmental fluctuations and stochasticity (L97-98), it would make sense to present a test of the importance of these processes to the model output. Would a simpler model provide similarly good results?

R: We believe that the main purpose of modelling is to illustrate the reality and serve as a tool for systematic assessment of the processes. Simple community models without individual-based processes implicitly weigh on generality and forgive outliers. However, environmental fluctuation and extremes are becoming more frequent and intensive with climate change, and this is likely to give advantage to an otherwise unlikely change in peatland community. To help with this situation, our modelling is able to populate outputs along a probability distribution and allows assessing individuals with different trait combinations as a part of the probabilities. As these models are fundamentally different in focuses and underlying mechanisms, simply comparing the goodness of results seems pointless.

My new comment: In this case I was not suggesting that you compare your model to previous, unrelated, models, but that you do tests with your own model, simplifying some processes and seeing if that degrades the results. E.g. instead of using realistic parameter distributions just use a

random number generator to e.g. modify the length growth of individual shoots (grid cells). Instead of using realistic environmental fluctuations just use the smoothed mean monthly climate. These are just some examples, I am sure you can think of better ones.

- We added Test 9-10 following the suggestions. In Test 9, we used smoothed monthly mean meteorological data to drive the model simulations. In Test 10, we eliminated the stochasticity in all model parameters and used only the mean values for simulation.

Continuation of my previous comment: I would also be interested in seeing the effects of the water retention and photosynthetic water-response parameters separately. Especially since the parameters for the latter may suffer from some measurement artefacts.

R: This is a very appreciated comment. Our future goal is also to make the picture clearer and understanding the factorial effects is a very important aspect. At the moment, our data and techniques are insufficient to separate the different effects. Therefore, model testing based on the parameters quantified by the “mixed” information could be less informative, unless we have had improved measurement data.

In addition, *S. fallax* and *S. magellanicum* are largely different in both water retention and photosynthetic response to water stress. Further testing on species either with similar water retention, or with similar photosynthetic response would be more informative to this question.

My new comment: In my mind, a model is the perfect opportunity to pretend that your species are not different in both but just in one or the other aspect and to test the individual effects of these parameters. You would not have real data to validate the result, but that is not the point here. The point is to understand what these parameters do and what would happen with hypothetical species with these parameter combinations. For me, this type of test is what would constitute a ‘systematic assessment of the processes’ (L189 in your response).

-Based on the suggestion, we simulated the mean cover of the two moss species by setting photosynthetic water-response parameters to be the same for both species but keep the water retention effects different (Test 7-8)

My new comment regarding my previous point 7: I did not mean to say that module III is unimportant, but it is not evaluated in this paper (just used to create input data for the presented model modules), so it seems too much (therefore unbalanced) to spend several pages on explaining the details of module III. I would recommend moving this information to the supplement.

- Moved to the supplements (as a part of Supplement A)

Additionally: Table 4, the sensitivity analysis: how do these 10% changes relate to the actual uncertainty in the parameter values?

-We used the 10% changes to test the parameter sensitivity, as we have limited information on the actual values of the parameters regarding to our site. Indeed, a change of 10% may not be comparable to the actual uncertainty of some parameter values (e.g. hydraulic conductivity of peat may vary by several orders, depending on the peat quality). However, the test for parameter sensitivity here aims to reveal the robustness of model at “current” states, rather than to investigate scenarios with different actual variations.

| 31

| 32

33

34 Modelling the habitat preference of two key *Sphagnum* species in a poor fen as controlled by
35 capitulum water ~~retention~~content

36 Jinnan Gong¹, Nigel Roulet², Steve Frohking^{1,3}, Heli Peltola¹, Anna M. Laine^{1,4}, Nicola
37 Kokkonen¹, Eeva-Stiina Tuittila¹

38 ¹ School of Forest Sciences, University of Eastern Finland, P.O. Box 111, FI-80101 Joensuu,
39 Finland

40 ² Department of Geography, McGill University and Centre for Climate and Global Change
41 Research, Burnside Hall, 805 rue Sherbrooke O., Montréal, Québec H3A 2K6

42 ³ Institute for the Study of Earth, Oceans, and Space, and Department of Earth Sciences,
43 University of New Hampshire, Durham, NH 03824, USA

44 ⁴ Department of Ecology and Genetics, University of Oulu, P.O. Box 3000, FI-90014, Oulu,
45 Finland

46

47 **Abstract**

48 Current peatland models generally ~~treat lack dynamic plant community structure~~vegetation as
49 ~~static~~, although ~~plant community structure is known to alter as a response to environmental~~
50 ~~change~~. ~~Because~~ the vegetation ~~dynamics-structure~~ and ecosystem functioning are tightly
51 linked. ~~R~~ realistic projections of peatland response to climate change requires including
52 vegetation dynamics in ecosystem models. In peatlands, *Sphagnum* mosses are key engineers.
53 ~~M~~The moss community composition primarily follows habitat moisture conditions. The species
54 known preference along the prevailing moisture gradient might not directly serve as a reliable
55 predictor for future species compositions as water table fluctuation is likely to increase. Hence,
56 modelling the mechanisms that control the habitat preference of *Sphagna* is a good first step for
57 modelling ~~the~~ community dynamics in peatlands. In this study, we developed the Peatland Moss
58 Simulator (PMS), ~~simulating community dynamics of the peatland moss layer~~a process-based
59 ~~model, for simulating community dynamics of the peatland moss layer that results in habitat~~
60 ~~preferences of Sphagnum species along moisture gradient~~. PMS ~~is a process-based model that~~
61 employs a ~~stochastic, n~~ individual-based approach ~~simulating competition within peatland moss~~
62 ~~layer based on species differences into describe the variation of functional traits among shoots~~
63 ~~and the stochastic base of competition~~. At the shoot-level, growth and competition were driven
64 by net photosynthesis, which was regulated by hydrological processes via capitulum water
65 ~~retention~~content. The model was tested by predicting the habitat preferences of *S. magellanicum*
66 and *S. fallax*, two key species representing dry (hummock) and wet (lawn) habitats in a poor fen
67 peatland (Lakkasuo, Finland). PMS successfully captured the habitat preferences of the two

68 *Sphagnum* species, based on observed variations in trait properties. Our model simulation further
69 showed that the validity of PMS depended on the interspecific differences in capitulum water
70 ~~retention-content~~ being correctly specified. Neglecting the water ~~retention-content~~ differences led
71 to the failure of PMS to predict the habitat preferences of the species in stochastic simulations.
72 Our work highlights the importance of capitulum water ~~content retention~~ to the dynamics and
73 carbon functioning of *Sphagnum* communities in peatland ecosystems. Studies of peatland
74 responses to changing environmental conditions thus need to include capitulum water processes
75 as a control on ~~the-moss community vegetation~~ dynamics. ~~For that e~~Our PMS model could be
76 used as an elemental design for the future development of dynamic vegetation models for
77 peatland ecosystems.

78

79 **Keywords:** *Sphagnum* moss; capitulum water content; competition; peatland community
80 dynamics; process-based modelling; moss traits; Peatland Moss Simulator (PMS)

81

82 1. Introduction

83 Peatlands have important roles in the global carbon cycle as they store about 30% of the world's
84 soil carbon (Gorham, 1991; Hugelius et al., 2013). Environmental changes, like climate warming
85 and land-use changes, are expected to impact the carbon functioning of peatland ecosystems
86 (Tahvanainen, 2011). Predicting the functioning of peatlands under environmental changes
87 requires models to quantify the interactions among ecohydrological, ecophysiological and
88 biogeochemical processes. These processes are known to be strongly regulated by vegetation
89 (Riutta et al. 2007; Wu and Roulet, 2014), which can change ~~during-over~~ decadal time
90 ~~scales~~ ~~frame~~ under changing hydrological conditions (Tahvanainen, 2011). ~~Current P~~peatland
91 models ~~have~~ generally ~~considered~~ ~~vegetation structure~~ ~~unrealistically as static component~~ ~~lack~~
92 ~~mechanisms for the dynamic plant community structure~~ (e.g. Frolking et al., 2002; Wania et al.,
93 2009) ~~that is unrealistic~~. ~~The recent regional-scale peatland model developed by Chaudhary et al.~~
94 ~~(2017) includes dynamic vegetation shifts among a single moss plant functional type (PFT) and~~
95 ~~four vascular PFTs-~~ ~~but to support realistic predictions on peatland functioning and global~~
96 ~~biogeochemical cycles~~ ~~Therefore, these mechanisms~~ ~~that drive changes in plant~~ ~~moss community~~
97 ~~structure~~ need to be identified and integrated with ecosystem processes, ~~in order to support~~
98 ~~realistic predictions on peatland functioning and the research community working on global~~
99 ~~biogeochemical cycles.~~

100 A major fraction of peatland biomass is formed by *Sphagnum* mosses (Hayward and Clymo,
101 1983; Vitt, 2000). Although individual *Sphagnum* species often have narrow habitat niches
102 (Johnson et al., 2015), different *Sphagnum* species replace each other along water table gradient
103 and therefore, as a genus, spread across a wide range of water table conditions (Rydin and

104 McDonald, 1985; Andrus et al. 1986; Rydin, 1993; Laine et al. 2009). The species composition
105 of the *Sphagnum* community strongly affects ecosystem processes such as carbon sequestration
106 and peat formation through interspecific variability in species traits such as photosynthetic
107 potential and ~~litter quality~~ (Clymo, 1970; O'Neill, 2000; Vitt, 2000; Turetsky, 2003). The
108 ~~*Sphagnum* production of biomass and litter~~ [production from *Sphagna*](#), which gradually raises the
109 moss carpet, ~~which feeds back into~~ [in turn affects](#) the species composition (Robroek et al.
110 2009). Hence, modelling the moss community dynamics is fundamental for predicting temporal
111 changes of peatland vegetation. As the distribution of *Sphagnum* species primarily follows the
112 variability in [peatland water table](#) ~~in a peatland~~ (Andrus 1986; Välranta et al. 2007), modelling
113 the habitat preference of *Sphagnum* species along a moisture gradient could be a good first step
114 for predicting moss community dynamics [in peatland ecosystems](#) (Blois et al., 2013).

115 For a given *Sphagnum* species, the optimal habitat represents the environmental conditions for
116 it to achieve higher rates of net photosynthesis and shoot elongation than ~~the its~~ peers (Titus &
117 Wagner, 1984; Rydin & McDonald, 1985; Rydin, 1997; Robroek et al., 2007a; Keuper et al.,
118 2011). Capitulum water content [and water storage](#), which is determined by the balance between
119 the evaporative loss and water gains from capillary rise and precipitation, represents one of the
120 most important controls on net photosynthesis (Titus & Wagner, 1984; Murray et al. 1989; Van
121 Gaalen et al. 2007; Robroek et al., 2009). To quantify the water processes in mosses,
122 hydrological models have been developed to simulate the water movement between moss carpet
123 and the peat underneath (~~Price, 2008; Price and Waddington, 2010~~), as regulated by the
124 variations in meteorological conditions and energy balance ([Price, 2008; Price and Waddington,](#)
125 [2010](#)). On the other hand, experimental work has addressed the species-specific responses of net
126 photosynthesis to changes in capitulum water content (Titus & Wagner, 1984; Hájek and
127 Beckett, 2008; Schipperges and Rydin, 2009) and light intensity (Rice et al., 2008; Laine et al.,
128 2011; Bengtsson et al., 2016). Net photosynthesis and hydrological processes are linked via
129 capitulum water retention, which controls the response of capitulum water content to water
130 potential changes (Jassey & Signarbieux, 2019). However, these mechanisms have not been
131 integrated with ecosystem processes in modelling. ~~Due to the lack of quantitative tools, the~~
132 ~~hypothetical importance of capitulum water retention has not yet been verified.~~

133 Along with the capitulum water processes, modelling the habitat preference of *Sphagna*
134 requires quantification of the competition among mosses, i.e., the “race for space” (Rydin, 1993;
135 Rydin, 1997; Robroek et al., 2007a; Keuper et al., 2011): *Sphagnum* shoots ~~can~~ form new
136 capitula and spread laterally, if there is space available. This reduces or eliminates the light
137 source for any plant that is buried by [its](#) peers (Robroek et al. 2009). As the competition occurs
138 between neighboring shoots, its modelling requires downscaling water-energy processes from
139 the ecosystem to the shoot level. For that, *Sphagnum* competition needs to be modelled as spatial
140 processes, considering that spatial coexistence and the variations of functional traits among shoot
141 individuals may impact the community dynamics (Bolker et al., 2003; Amarasekare, 2003).

142 However, coexistence generally relies on simple coefficients to describe the interactions among
143 individuals (e.g. Czárán and Iwasa, 1998; Anderson and Neuhauser, 2000; Gassmann et al.,
144 2003; Boulangeat et al., 2018), thus being decoupled from environmental fluctuation or the
145 stochasticity of biophysiological processes.

146 This study aims to develop and test a model, the Peatland Moss Simulator (PMS), to simulate
147 community dynamics within the peatland moss layer that results in realistic habitat preference of
148 *Sphagnum* species along a moisture gradient. In PMS, community dynamics is driven by
149 *Sphagnum* photosynthesis. ~~Photosynthesis in turn is regulated by capitulum water retention~~
150 ~~through capitulum moisture content~~. Therefore, we hypothesize that water retention of the
151 capitula is the mechanism driving moss community dynamics. We test the model validity using
152 data from an experiment based on two *Sphagnum* species with different positions along moisture
153 gradient in the same peatland site. If our hypothesis holds, the model will (1) correctly predict
154 the competitiveness of the two species in wet and dry habitats; and (2) fail to predict
155 competitiveness if the capitulum water retention and water content of the two species are not
156 correctly specified.

157

158 2. Materials and methods

159 2.1 Study site

160 The peatland site being modelled is locateds in Lakkasuo, Orivesi, Finland (61° 47' N; 24° 18'
161 E). The site is a poor fen fed by mineral inflows from a nearby esker (Laine et al 2004). Most of
162 the site is formed by lawns dominated by *Sphagnum recurvum* complex (*Sphagnum fallax*,
163 accompanied by *Sphagnum flexuosum* and *Sphagnum angustifolium*) and *Sphagnum papillosum*.
164 Less than 10% of surface ares occupied by hummocks, with *Sphagnum magellanicum* and
165 *Sphagnum fuscum*, which are being 15-25 cm higher than the lawn surfaces ~~with *Sphagnum*~~
166 ~~*magellanicum* and *Sphagnum fuscum*~~. Both microforms are covered by continuous *Sphagnum*
167 carpet with a sparse cover of vascular plants (projection cover of *Carex* 12% on average), which
168 spread homogeneously over the topography. The annual mean water table was 15.6 ± 5.0 cm
169 deep ~~from~~ at lawn surface (Kokkonen et al., 2019). More information about the site can be found
170 in Kokkonen et al. (2019).

171

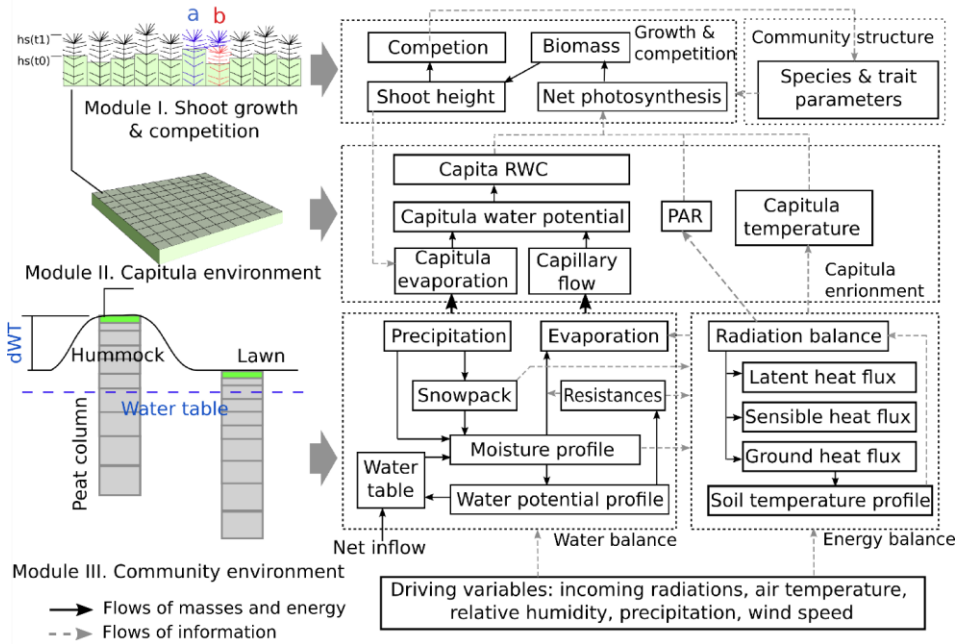
172 2.2 Model outline

173 The Peatland Moss Simulator (PMS) is a process-based, stochastic model, which simulates the
174 temporal dynamics of *Sphagnum* community as driven by variations in precipitation, irradiation,
175 and energy flow and with individual-based interactions (Fig. 1). In PMS, the studied ecosystem is
176 seen as a dual-column system consisting of hydrologically connected habitats of hummocks and

177 lawns (community environment in Fig. 1). For each habitat type, the community area is
178 downscaled to two-dimensional cells representing the scale of individual shoots (i.e. 1 cm²).
179 Each grid cell can be occupied by one capitulum from a single *Sphagnum* species. The
180 community dynamics, i.e. the changes in species abundances, are driven by the growth and
181 competition of *Sphagnum* shoots at the grid-cell level (Module I in Fig. 1). These processes were
182 regulated by the grid-cell-specific conditions of water and energy (Module II in Fig. 1), which
183 are derived from the community environment (Module III in Fig. 1).

184 In this study, we focused on developing Module I and II (Section 2.3) and employed an
185 available soil-vegetation-atmosphere transport (SVAT) model (Gong et al., 2013a, 2016) to
186 describe the water-energy processes for Module III (Appendix A). We assumed that the temporal
187 variation in water table was similar in lawns and hummocks, and the hummock-lawn differences
188 in water table (dWT in Fig. 1) followed their difference in surface elevations (Wilson, 2012). At
189 the grid cell level, the photosynthesis of capitula drove the biomass growth and elongation of
190 shoots, which led to the ~~“race for space”~~ “competition” between adjacent grid cells. The net
191 photosynthesis rate was controlled by capitulum water content (W_{cap}), which was defined by the
192 capitulum water retention in relation to water potential (h) (Section 2.4). The values for
193 functional traits that regulate the growth and competition processes were randomly selected
194 within their normal distribution measured in the field (Section 2.4). Unknown parameters that
195 related the lateral water flows of the site are estimated using a machine-learning approach
196 (Section 2.5). Finally, Monte-Carlo simulation was used to support the analysis on the habitat
197 preferences of *Sphagnum* species and hypothesis tests (Section 2.6). The list of used symbols is
198 given in Table 1.

199



200

201 Fig. 1 Framework of Peatland Moss Simulator (PMS).

202

203 2.3 Model development

204 2.3.1 Calculating shoot growth and competition of Sphagnum mosses (Module I)

205 Calculation of Sphagnum growth

206 To model grid cell biomass production and height increment, we assumed that capitula were the
 207 main parts of shoots responsible for photosynthesis and production of new tissues, instead of the
 208 stem sections underneath. We employed a hyperbolic light-saturation function (Larcher, 2003) to
 209 calculate the net photosynthesis, which was parameterized based on empirical measurements
 210 made from the target species collected from the study site (see Appendix B for materials and
 211 methods):

$$212 A_{20} = \left(\frac{Pm_{20} * PPFD}{\alpha_{PPFD} + PPFD} - Rs_{20} \right) * B_{cap} \quad (1)$$

213 where subscript 20 denotes the variable value measured at 20 °C; R_s is the mass-based
 214 respiration rate ($\mu\text{mol g}^{-1} \text{s}^{-1}$); Pm is the mass-based rate of maximal gross photosynthesis (μmol
 215 $\text{g}^{-1} \text{s}^{-1}$); $PPFD$ is the photosynthetic photon flux density ($\mu\text{mol m}^{-2} \text{s}^{-1}$); B_{cap} is the capitulum

216 **biomass**; and α_{PPFD} is the half-saturation point ($\mu\text{mol m}^{-2} \text{s}^{-1}$) for photosynthesis.

217 By adding multipliers for capitula water content (f_w) and temperature (f_T) to Eq. (1), the net
218 photosynthesis rate A ($\mu\text{mol m}^{-2} \text{s}^{-1}$) was calculated as following:

$$219 \quad A = \left[\frac{Pm_{20} * PPFD}{\alpha_{PPFD} + PPFD} f_T(T) - Rs_{20} f_R(T) \right] * B_{cap} * f_w(W_{cap}) \quad (2)$$

220 where $f_w(W_{cap})$ describes the responses of A to capitulum water content, W_{cap} ; $f_T(T)$ describes
221 the responses of Pm to capitulum temperature T (Korrensalo et al., 2017). $f_w(W_{cap})$ was estimated
222 based on the empirical measurements (Appendix B; see Section 2.4). The temperature response
223 $f_R(T)$ is a Q_{10} function that describes the temperature sensitivity of Rs (Frolking et al., 2002):

$$224 \quad f_R(T) = Q_{10}^{(T - T_{opt})/10} \quad (3)$$

225 where Q_{10} is the sensitivity coefficient; T is the capitulum temperature ($^{\circ}\text{C}$); T_{opt} (20°C) is the
226 reference temperature of respiration.

227 The response of A to W_{cap} ($f_w(W_{cap})$, Eq. 2) was described as a second-order polynomial
228 function):

$$229 \quad f_w(W_{cap}) = a_{w0} + a_{w1} * W_{cap} + a_{w2} * W_{cap}^2 \quad (4)$$

230 where a_{w0} , a_{w1} and a_{w2} are coefficients.

231 Plants can store carbohydrates as nonstructural carbon (NSC, e.g. starch and soluble sugar) to
232 support fast growth in spring or post-stress periods, like after drought events (Smirnoff et al.,
233 1992; Martínez-Vilalta et al., 2016; Hartmann and Trumbore, 2016). We linked the production of
234 shoot biomass to the immobilization of NSC storage (modified from Eq. 10 in Asaeda and
235 Karunaratne, 2000). The change in NSC storage depends on the balance between net
236 photosynthesis and immobilization:

$$237 \quad M_B = s_{imm} * NSC * k_{imm} \alpha_{imm}^{T-20} \quad (5)$$

$$239 \quad \partial NSC / \partial t = A - M_B, NSC \in [0, NSC_{max}] \quad (6)$$

240 where M_B is the immobilized NSC to biomass production during a time step (g); k_{imm} is the
241 specific immobilization rate (g g^{-1}) (Asaeda and Karunaratne 2000); α_{imm} is the temperature
242 constant; s_{imm} is the multiplier for temperature threshold, where $s_{imm} = 1$ when $T > 5^{\circ}\text{C}$ but $s_{imm} =$
243 0 if $T \leq 5^{\circ}\text{C}$. NSC_{max} is the maximal NSC concentration in *Sphagnum* biomass (Turetsky et al.,
244 2008). Timing of growth is controlled by a temperature threshold and NSC availability. Growth
245 occurs when $T > 5^{\circ}\text{C}$ and NSC is above zero. The dynamics of NSC storage are related to WC
246 through net photosynthesis.

247 The increase in shoot biomass drove the shoot elongation:

248 $\partial Hc / \partial t = \frac{M_B}{H_{spc} S_c}$ (7)

249 where Hc is the shoot height (cm); H_{spc} is the biomass density of *Sphagnum* stems ($\text{g m}^{-2} \text{cm}^{-1}$)
 250 and S_c is the area of a cell (m^2).

251

252 *Calculation of Sphagnum competition and community dynamics*

253 To simulate the competition among *Sphagnum* shoots, we first compared Hc of each grid cell
 254 (source grid cell, i.e. grid cell a in Fig. 1) to its four neighboring cells and marked the one with
 255 lowest position (e.g. grid cell b in Fig. 1) as the target of spreading. The spreading of shoots from
 256 a source to a target grid cell occurred when the following criteria were fulfilled: i) the height
 257 difference between source and target grid cells exceeded a threshold value; ii) NSC accumulation
 258 in the source grid cell was large enough to support the growth of new capitula in the target grid
 259 cell; iii) the capitula in the source grid cell can split at most once per year.

260 The threshold of height difference in rule i) was set equal to the mean diameter of capitula in
 261 the source cell, based on the assumption that the shape of a capitulum was spherical. When
 262 shoots spread, the species type and model parameters in the target grid cell were overwritten by
 263 those in the source grid cell, assuming the mortality of shoots originally in the target cell. During
 264 the spreading, NSC storage was transferred from the source cell to the target cell to form new
 265 capitula. In cases where spreading did not take place, establishment of new shoots from spores
 266 ~~was allowed to~~ could maintain the continuity of *Sphagnum* carpet at the site. During the
 267 establishment from spores, which was rare and occurred during the first years of simulation, the
 268 ~~properties—traits~~ of *Sphagnum* species were randomized within their normal distribution
 269 measured in the field.

270

271 **2.3.2 Calculating grid cell-level dynamics of environmental factors (Module II)**

272 Module II computes grid-cell values of W_{cap} , $PPFD$ and T for Module I. The cell-level $PPFD$
 273 and T were assumed to be equal to the community means, which were solved by the SVAT
 274 scheme in Module III (Appendix A.). The community level evaporation rate (E) was partitioned
 275 to cell-level (E_i) as following:

276 $E_i = E * \left(\frac{Sv_i}{r_{bulk,i}} \right) / \sum \left(\frac{Sv_i}{r_{bulk,i}} \right)$ (8)

277 where $r_{bulk,i}$ is the bulk surface resistance of cell i , which is as a function ($r_{bulk,i} = fr(h_i)$) of grid-
 278 cell-based water potential h_i , capitulum biomass (B_{cap}) and shoot density (D_S) based on the
 279 empirical measurements (Appendix B); Sv_i was the evaporative area, which was related to the
 280 height differences among adjacent grid cells:

281
$$Sv_i = Sc_i + lc \sum_j (Hc_i - Hc_j) \quad (9)$$

282 where lc is the width of a grid cell (cm); and subscript j denotes the four-nearest neighbouring
 283 grid cells. In this way, changes in the height difference between the neighboring shoots feeds
 284 back to affect the water conditions of the grid cells, via alteration of the evaporative surface area.

285 The grid cell-level changes in capitula water potential (h_i) ~~were~~ driven by the balance
 286 between the evaporation (E_i) and the upward capillary flow to capitula:

287
$$\partial h_i = \frac{K_m}{C_i} \left[\frac{(h_i - h_m)}{0.5z_m} - 1 - E_i \right] \quad (10)$$

288 where h_m is the water potential of the living moss layer, solved in Module III (Appendix A.); z_m
 289 is the thickness of the living moss layer ($z_m=5$ cm); K_m is the hydraulic conductivity of the moss
 290 layer and that is set to be the same for each grid cell; C_i is the cell-level specific water uptake
 291 capacity ($C_i = \partial W_{cap,i} / \partial h_i$). $\partial W_{cap,i} / \partial h_i$ could be derived from the capitulum water retention
 292 function $h_i = f_h(W_{cap})$. W_{cap} can be then calculated from the estimated from h_i and affect the
 293 calculation of net photosynthesis through $f_w(W_{cap})$ (Eq. 2).

294

295 **2.4 Model parameterization**

296 *Selection of Sphagnum species*

297 We chose *S. fallax* and *S. magellanicum*, which form 63% of total plant cover at the study site at
 298 Lakkasuo (Kokkonen et al., 2019), as the target species representing the lawn and hummock
 299 habitats respectively. These species share a similar niche along the gradients of soil pH and
 300 nutrient richness (Wojtuń et al., 2003), but are discriminated by their preferences of water table
 301 level (Laine et al., 2004). While *S. fallax* is commonly found close to the water table (Wojtuń et
 302 al., 2003), *S. magellanicum* can occur along a wider range of a dry-wet gradient, from
 303 intermediately wet lawns up to dry hummocks (Rice et al., 2008; Kyrkjeeide, et al., 2016;
 304 Korresalo et al., 2017). The transition from *S. fallax* to *S. magellanicum* along the wet-dry
 305 gradient thus indicates the decreasing competitiveness of *S. fallax* against *S. magellanicum* with
 306 a lowering water table.

307 *Parameterization of morphological traits, net photosynthesis and capitulum water retention*

308 We empirically quantified the morphological traits capitulum density (D_s , shoots cm^{-2}), biomass
 309 of capitula (B_{cap} , g m^{-2}), biomass density of living stems (H_{spc} , $\text{g cm}^{-1} \text{m}^{-2}$), net photosynthesis
 310 parameters (Pm_{20} , Rs_{20} and α_{PPFD}) and the water retention properties (i.e., $f_h(W_{cap})$ and $fr(h)$), Eqs.
 311 8 and 10) for the two *Sphagnum* selected species ~~from the same site~~ (see Appendix B for
 312 methods). The values (mean \pm SD) of the morphological parameters, the photosynthetic
 313 parameters and polynomial coefficients (a_{w0} , a_{w1} and a_{w2} , Eq. 3) are listed in Table 2. For each
 314 parameter, a random value was initialized for each cell based on the measured means and SD,

315 assuming the variation of parameter values is normally distributed.

316 We noticed that the fitted $f_W(W_{cap})$ was meaningful when W_{cap} was below the optimal water
317 content for photosynthesis ($W_{opt} = -0.5 a_{W1}/ a_{W2}$). If $W_{cap} > W_{opt}$, photosynthesis decreased
318 linearly with increasing W_{cap} , as being limited by the diffusion of CO₂ (Schipperges and Rydin,
319 1998). In that case, $f_W(W_{cap})$ was calculated following Frolking et al. (2002):

$$320 \quad f_W(W_{cap}) = 1 - 0.5 \frac{W_{cap} - W_{opt}}{W_{max} - W_{opt}} \quad \text{—————}$$

321 (11)

322 where W_{max} is the maximum water content of capitula.

323 It is known that W_{max} is around 25-30 g g⁻¹ (e.g. Schipperges and Rydin, 1998), or about 0.31 -
324 0.37 cm³ cm⁻³ in term of volumetric water content (assuming 75 g m⁻² capitula biomass and 0.6
325 cm height of capitula layer). This range is broadly lower than the saturated water content of moss
326 carpet (> 0.9 cm³ cm⁻³, McCarter and Price, 2014). Consequently, we used the following
327 equation to convert volumetric water content to capitula RWC, when h_i was higher than the
328 boundary value of -10^4 cm:

$$329 \quad W_{cap} = \min(W_{max}, \theta_m / (H_{cap} * B_{cap} * 10^{-4})) \quad \text{—————}$$

330 (12)

331 where W_{max} is the maximum water content that set to 25 g g⁻¹ for both species; θ_m is the
332 volumetric water content of moss layer; H_{cap} is the height of capitula and is set to 0.6 cm (Hájek
333 and Beckett, 2008).

334 *Parameterization of SVAT processes*

335 ~~For the calculation of surface energy balance, we set the height and leaf area of vascular~~
336 ~~canopy to 0.4 m and 0.1 m² m⁻², consistent with the scarcity of vascular canopies at the site. The~~
337 ~~aerodynamic resistance (r_{aeros} , Eq. A14, Appendix A) for surface energy fluxes was calculated~~
338 ~~following Gong et al. (2013a). The bulk surface resistance of community (r_{sv} , Eq. A13, Appendix~~
339 ~~A) was summarized from the cell level values of $r_{bulk,i}$, that $1/r_{sv} = \sum(1/r_{bulk,i})$. To calculate the~~
340 ~~peat hydrology and water table, peat profiles of hummock and lawn communities were set to 150~~
341 ~~cm deep and stratified into horizontal layers of depths varying from 5cm (topmost) to 30cm~~
342 ~~(deepest). For each peat layer, the thermal conductivity (K_T) of fractional components, i.e. peat,~~
343 ~~water and ice, were evaluated following Gong et al. (2013a). The bulk density of peat (ρ_{bulk}) was~~
344 ~~set to 0.06 g cm⁻³ below acrotelm (40 cm depth, Laine et al., 2004), and decreased linearly~~
345 ~~toward the living moss layer. The saturated hydraulic conductivity (K_{sat} , Eq. A6, Appendix A)~~
346 ~~and water retention parameters (i.e. α and n , Eq. A5, Appendix A) of water retention curves were~~
347 ~~calculated as functions of ρ_{bulk} and the depth of peat layer following Päivänen (1973). K_{sat} , α and~~
348 ~~n for the living moss layer were adopted from the values measured by McCarter and Price (2014)~~

349 from *S. magellanicum* carpet. The parameter values for SVAT processes are listed in Table 3.

350 *Calculation of snow dynamics*

351 In boreal and arctic regions, the amount and timing of snow melt has crucial impact on moisture
352 conditions, especially at fen peatlands. Therefore, to have realistic spring conditions we
353 introduced a snow pack model, SURFEX v7.2 (Vionnet et al., 2007), into the SVAT modelling.
354 The snow pack model simulates snow accumulation, wind drifting, compaction and changes in
355 metamorphism and density. These processes influenced the heat transport and freezing melting
356 processes (i.e. S_L and S_T , see Eq. A1-A2, Appendix A). In this modelling, we calculate the snow
357 dynamics on a daily basis in parallel to the SVAT simulation. Daily snowfall was converted into
358 a snow layer and added to ground surface. For each of the day based snow layers (D layers), we
359 calculated the changes in snow density, particle morphology and layer thicknesses. At each time
360 step, D layers were binned into layers of 5–10 cm depths (S layers) and placed on top of the peat
361 column for SVAT modelling. With a snow layer present, surface albedos (i.e. a_s , a_t) were
362 modified to match those of the topmost snow layer (see Table 4 in Vionnet et al., 2007). If the
363 total thickness of snow was less than 5 cm, all D layers were binned into one S layer. The
364 thermal conductivity (K_T), specific heat (C_T), snow density, thickness and water content of each
365 S layer were calculated as the mass weighted means from the values of D layers. Melting and
366 refreezing tended to increase the density and K_T of a snow layer but decrease its thickness (see
367 Eq. 18 in Vionnet et al., 2007). The fraction of melted water that exceeded the water holding
368 capacity of a D layer (see Eq. 19 in Vionnet et al., 2007) was removed immediately as
369 infiltration water. If the peat layer underneath was saturated, the infiltration water was removed
370 from the system as lateral discharge.

371 *Boundary conditions and driving variables*

372 A zero flow boundary was set at the bottom of peat. At peat surface the boundary conditions of
373 water and energy were defined by the ground surface temperature (T_0 , see Eq. A10–A15 in
374 Appendix A) and the net precipitation (P minus E). The profiles of layer thicknesses, ρ_{bulk} and
375 hydraulic parameters were assumed to be constant during simulation. Lateral boundary
376 conditions were used to calculate the spreading of *Sphagnum* shoots among cells along the edge
377 of the model domain so that shoots can spread across the edge of simulation area and invade into
378 the grid cell at the boarder of the opposite side.

379 The model simulation was driven by climatic variables of air temperature (T_a), precipitation
380 (P), relative humidity (Rh), wind speed (u), incoming shortwave radiation (R_s) and longwave
381 radiation (R_l). To support the stochastic parameterization of the model and Monte Carlo
382 simulations, Weather Generator (Strandman et al., 1993) was used to generate randomized
383 scenarios based on long term weather statistics (period of 1981–2010) from 4 closest weather
384 stations of Finnish Meteorological Institute. This generator had been intensively tested and
385 applied under Finnish conditions (Kellomäki and Väisänen, 1997; Venäläinen et al., 2001; Alm

386 ~~et al., 2007). We also compared the simulated meteorological variables against 2-year data~~
387 ~~measured from Siikaneva peatland site (61°50 N; 24°10 E), located 10 km away from our study~~
388 ~~site (Appendix C).~~

389

390 2.5 Model calibration for lateral water influence

391 We used a machine-learning approach to estimate the influence of upstream area on the water
392 balance of the site. The rate of net inflow (I , see Eq. A18 in Appendix A.) was described as a
393 function of Julian day (JD), assuming the inflow was maximum after spring thawing and then
394 decreased linearly with time:

$$395 I_j = (a_N * JD + b_N) * Ks_j, JD > JD_{thaw} \quad (11)$$

396 where subscript j denotes the peat layers under water table; Ks is the saturated hydraulic
397 conductivity; JD_{thaw} is the Julian day that thawing completed; and a_N and b_N are parameters.

398 We simulated water table changes using climatic scenarios from the Weather Generator (Section
399 2.4 Appendix A). During the calibration, the community compositions were set constant, such
400 that *S. magellanicum* fully occupied the hummock habitat whereas *S. fallax* fully occupied the
401 lawn habitat. The simulated multi-year means of weekly water table values were compared to the
402 weekly mean water table obtained observed at the site during years 2001, 2002, 2004 and 2016.
403 The cost function for the learning process was based on the sum of squared error (SE) of the
404 simulated water table:

$$405 SE = \sum (WTS_k - WTM_k)^2 \quad (12)$$

406 where WTm is the measured multi-year weekly mean of water table; WTS is the simulated multi-
407 year weekly mean of water table; and subscript k denotes the week of year when the water table
408 was sampled.

409 The values of a_N and b_N were estimated using the Gradient Descent approach (Ruder, 2016),
410 by minimizing SE in above Eq. (19):

$$411 X_N(j) = X_N(j) - \Gamma \frac{\partial SE}{\partial X_N(j)} \quad (13)$$

412 where Γ is the learning rate ($\Gamma = 0.1$). Appendix D shows the simulated water table with the
413 calibrated inflow term I , as compared against the measured values from the site.

414

415

416 2.6 Model-based analysis

417 First, we examined the ability of model to capture the preference of *S. magellanicum* for the
418 hummock environment and *S. fallax* for the lawn environment (Test 1). For both species, the
419 probability of occupation was initialized as 50% in a cell, and the distribution of species in the
420 communities were randomly patterned. Monte-Carlo simulations (40 replicates) were carried out,
421 with a time step of 30 minutes. A simulation length of 15 years was selected based on
422 preliminary studies, in order to cover the major ~~part-interval~~ of change and ~~to ease the~~
423 computational demand. Biomass growth, stem elongation and the spreading of shoots were
424 simulated on a daily basis. The establishment of new shoots in deactivated cells was calculated at
425 the end of each simulation year. We then assessed if the model could capture the dominance of *S.*
426 *magellanicum* in the hummock communities and the dominance of *S. fallax* in lawn
427 communities. The simulated annual height increments of mosses were compared to the values
428 measured for each community type. To measure moss height growth in the field, we deployed 20
429 cranked wires on *S. magellanicum* dominated hummocks and 15 on *S. fallax* dominated lawns in
430 2016. Each cranked wire was a piece of metal wire attached with plastic brushes at the side
431 anchored into the moss carpet (e.g. Clymo 1970, Holmgren et al., 2015). Annual height growth
432 (dH) was determined by measuring the change in the exposed wire length above moss surface
433 from the beginning to the end of growing season.

434 Second, we tested the robustness of the model to the uncertainties in a set of parameters (Test
435 2-4). In test 2, we focused on parameters that closely linked to hydrology and growth
436 calculations, but were roughly parameterized (e.g. k_{imm} , r_{aero}) or adopted as a prior from other
437 studies (e.g. K_{sat} , α , n , NSC_{max} ; see Table 3). One at a time, each parameter value was adjusted
438 by +10 % or -10 %, and species cover was simulated using the same runtime settings as Test 1
439 with 40 Monte Carlo runs. The simulated means of cover were then compared to those
440 calculated without the parameter adjustment. 40 Monte-Carlo simulations were run using the
441 same runtime settings as in Test 1. The simulated means of cover were then compared to those
442 calculated without the parameter adjustment.

443 Tests 3-4 were then carried out to test whether the model could correctly predict
444 competitiveness of the species in dry and wet habitats, if the species-specific trends of capitulum
445 water ~~retention-content~~ were not correctly specified. For both species, we set the values of
446 parameters controlling the water retention (i.e. B_{cap} and D_s , Appendix B) and the water-stress
447 effects on net photosynthesis (i.e. W_{cap} , Eq. 4) to be the same as those in *S. magellanicum* (Test
448 3) or same as those in *S. fallax* (Test 4). Our hypothesis would be supported if removing the
449 interspecific differences in RWC responses led to the failure to predict the habitat preferences of
450 the species.

451 We implemented Tests 5-6 to test the importance of parameters that directly control the species
452 ability to overgrow another species with more rapid height increment (i.e. Pm_{20} , RS_{20} , α_{PPFD} and
453 H_{spec}) in lawn and hummock conditions. We eliminated the species differences in the parameter

454 values to be same as those in *S. magellanicum* (Test 5) and same as those in *S. fallax* (Test 6).
455 The effects of the manipulation were compared against those from Tests 3-4. For each of Tests
456 3-6, 80 Monte-Carlo simulations were run using the setups described in Test 1.

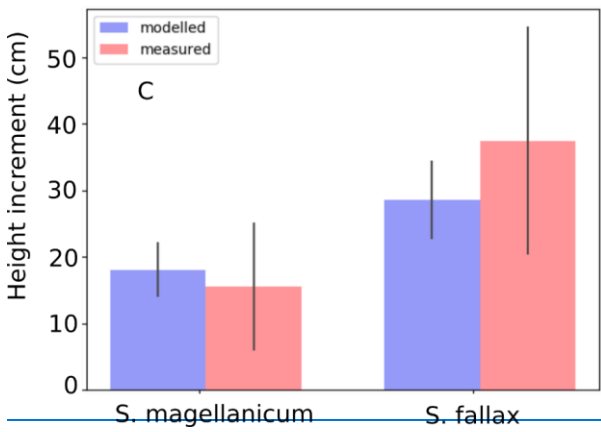
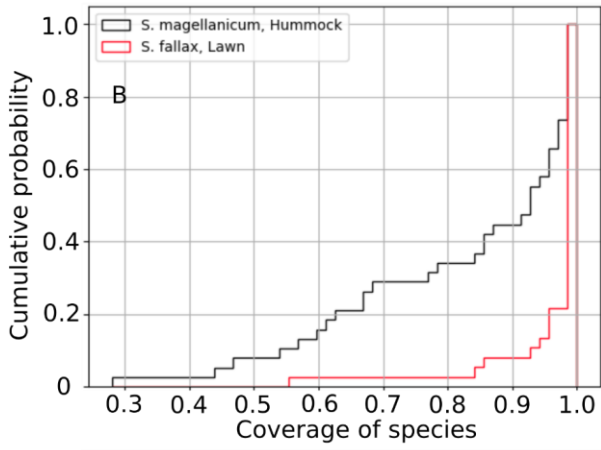
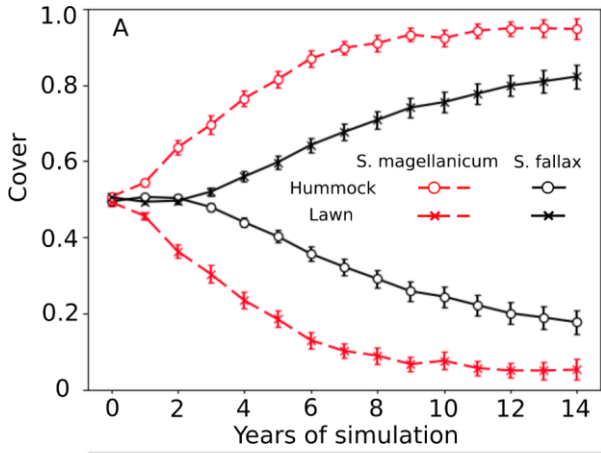
457 Test 7-8 were implemented to separate the effects of photosynthetic water-response
458 parameters from the effects of the water retention of capitula. We set the photosynthetic water-
459 response parameters to be the same as those in *S. magellanicum* (Test 7) and same as those in *S.*
460 *fallax* (Test 8). As our model aimed to couple the environmental fluctuations and stochasticity of
461 ecosystem processes, we further tested the model responses to the absences of environmental
462 fluctuations (Test 9) or the absence of stochasticity in model parameters (Test 10). In Test 9,
463 monthly mean values of meteorological variables were used to drive the model simulation. In
464 Test 10, we removed the stochasticity of model parameters, and assigned average value to each
465 parameter of grid cells. For each of Tests 7-10, 40 Monte-Carlo simulations were run using the
466 setups described in Test 1.

467
468

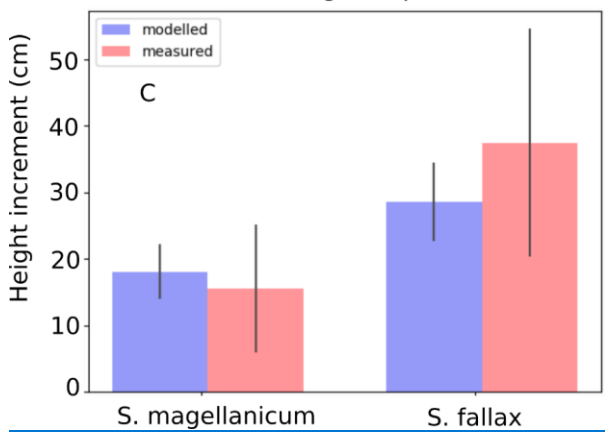
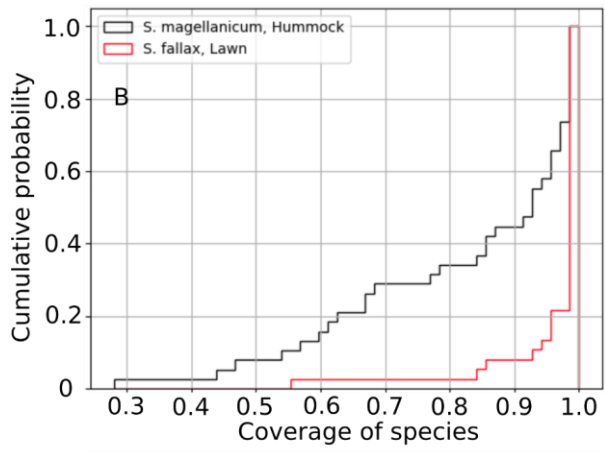
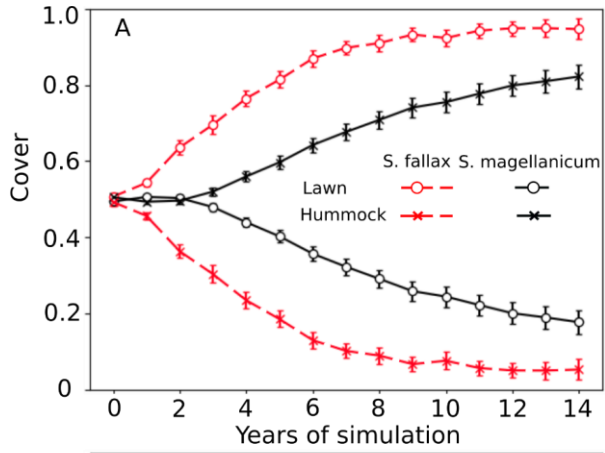
469 **3 Results**

470 **3.1 Simulating the habitat preferences of *Sphagnum* species as affected by water retention**
471 **content traits of capitulum**

472 Test 1 ~~showed~~ demonstrated the ability of model to capture the preference of *S. magellanicum*
473 for the hummock environment and *S. fallax* for the lawn environment (Fig. 2A). The simulated
474 annual changes in species covers were greater in lawn than in hummock habitats during the first
475 5 simulation years. The changes in lawn habitats slowed down around year 10 and the cover of *S.*
476 *fallax* plateaued at around $95 \pm 2.8\%$ (mean \pm standard error). In contrast, the cover of *S.*
477 *magellanicum* on hummocks continued to grow until the end of simulation and reached
478 $83 \pm 3.1\%$. In the lawn habitats, the cover of *S. fallax* increased in all Monte-Carlo simulations
479 and the species occupied all grid cells in 70% of the simulations. In the hummock habitats, the
480 cover of *S. magellanicum* increased in 91% of Monte-Carlo simulations, and formed
481 monocultural community in 16% of simulations (Fig. 2B). The height growth of *Sphagnum*
482 mosses was significantly greater at lawns than at hummocks ($P < 0.01$). The ranges of simulated
483 height growths agreed well with the observed values from field measurement for both species
484 (Fig. 2C).



485



487 Figure 2. Testing the ability of PCSMS to predict habitat preference of *Sphagnum magellanicum*
488 and *S. fallax* (Test 1). The hummock and lawn habitats were differentiated by water table depth,
489 surface energy balances and capitulum water potential in modelling. In the beginning of
490 simulation, the cover of the two species was set equal and it was allowed to develop with time.
491 (A) Annual development of the relative cover (mean and standard error) of the two species in
492 hummock and lawn habitats, (B) the cumulative probability distribution of the cover of the two
493 species at the end of the 15-year period based on ~~4080~~ Monte-Carlo simulations, and (C) the
494 simulated and measured means of annual height growth of *Sphagnum* surfaces in their natural
495 habitats in hummock and lawn habitats.

496

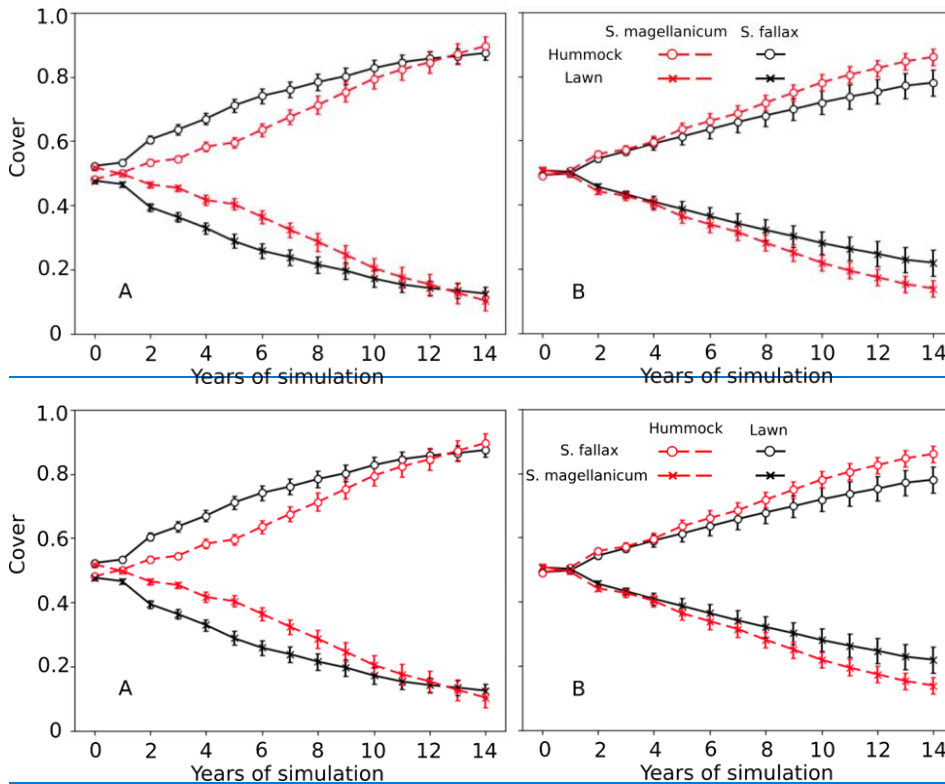
497 3.2 Testing model robustness

498 Test 2 addressed the model robustness to the uncertainties in several parameters that closely
499 linked to hydrology and growth calculations. Modifying most of the parameter values by +10%
500 or -10% yielded marginal changes in the mean cover of species in either hummock or hollow
501 habitat (Table 4). Reducing the moss carpet and peat hydraulic parameter n had stronger impacts
502 on *S. fallax* cover in hummocks than in lawns. Nevertheless, changes in simulated cover that
503 were caused by parameter manipulations were generally smaller than the standard deviations of
504 the means i.e. fitting into the random variation.

505

506 3.3 Testing the controlling role of capitulum water ~~retention-content~~ for community 507 dynamics

508 In Tests 3 and 4, the model incorrectly predicted the competitiveness of two species when the
509 interspecific differences of capitulum water ~~retention-content~~ were eliminated. In both tests, *S.*
510 *fallax* became dominant in all habitats. The use of water responses characteristic to *S.*
511 *magellanicum* for both species (Test 3) led to faster development of *S. fallax* cover and higher
512 coverage at the end of simulation (Fig. 3A), as compared with the simulation results where the
513 water responses characteristic to *S. fallax* were used for both species (Test 4, Fig. 3B). The
514 pattern was more pronounced in hummock than in lawn habitats.



515

516

517 Figure 3. Testing the importance of capitulum water ~~retention content~~ to the habitat preference of
 518 *S. magellanicum* and *S. fallax*. The development of the relative cover (mean and standard error)
 519 were simulated in hummock and lawn habitats over a 15-year time frame for the two species. For
 520 both species, parameter values for the capitulum water ~~retention content~~, capitulum biomass
 521 (B_{cap}) and density (D_s) were set to be the same as those from (A) *S. magellanicum* (Test 3) or (B)
 522 *S. fallax* (Test 4).

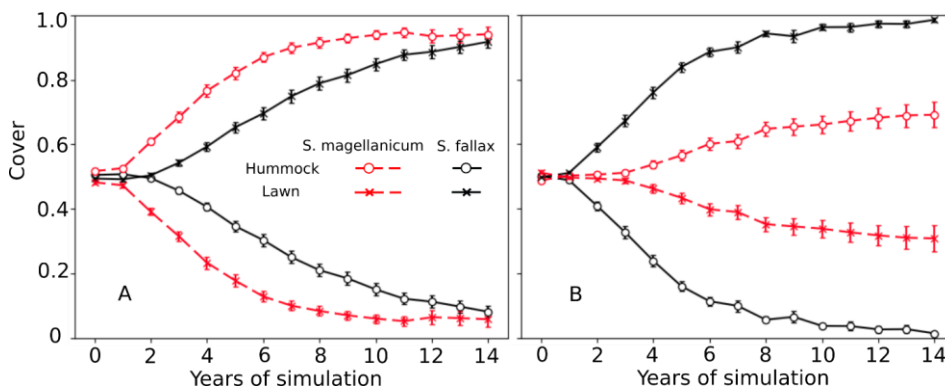
523

524 In Tests 5 and 6, the species differences in the growth-related parameters were eliminated.
 525 However, the model still predicted the dominances of *S. fallax* and *S. magellanicum* in lawn and
 526 hummock habitats, respectively (Fig. 4). The increase in the mean cover of *S. magellanicum* was
 527 especially fast in hummock habitat in comparison to the results of the unchanged model from
 528 Test 1 (Fig. 2A). In lawns, the use of *S. fallax* growth parameters for both species gave stronger
 529 competitiveness to *S. magellanicum* (Fig. 4B) than using the *S. magellanicum* parameters (Fig.
 530 4A). [In Test 7 and 8, ignoring the interspecific differences in the photosynthetic water-response](#)

531 [parameters did not change the simulated habitat preferences of *S. fallax* and *S. magellanicum*](#)
 532 [\(Table 5\). Using the water response parameters of *S. fallax* decreased the mean cover of *S. fallax*](#)
 533 [in lawns but increased the cover of *S. magellanicum* on hummocks. In contrast, using the water](#)
 534 [response parameters of *S. magellanicum* increased the mean cover of *S. fallax* in lawns but](#)
 535 [decreased the cover of *S. magellanicum* on hummocks.](#)

536

537



538

539 Figure 4. Testing the importance of parameters regulating net photosynthesis and shoot
 540 elongation to the habitat preference of *S. magellanicum* and *S. fallax*. Annual development of the
 541 relative cover (mean and standard error) of the two species were simulated for hummock and
 542 lawn habitats over a 15-year time frame. For both species, the parameter values (i.e. Pm_{20} , Rs_{20} ,
 543 α_{PPFD} and H_{spec}) were set to be the same as those from (A) *S. magellanicum* (Test 5) or (B) *S.*
 544 *fallax* (Test 6).

545

546 [3.4 Testing the effects of environmental fluctuations and stochasticity of ecosystem](#)
 547 [processes on community dynamics](#)

548 [In Tests 9, the model failed to simulate the preference of *S. magellanicum* to hummocks \(Table](#)
 549 [5\) if the environmental fluctuation was ignored. However, the simulated cover of *S. fallax* in](#)
 550 [lawns was higher as compared to unchanged condition \(i.e. Test 1\). Using mean value for each](#)
 551 [model parameters led to mono output, i.e. *S. magellanicum* occupied 100% hummock area](#)
 552 [whereas *S. fallax* took over lawns completely.](#)

553

554

555 4 Discussion

556 In peatland ecosystems, ~~*Sphagnum*~~ *Sphagna* are keystone species ~~differentially~~ distributed
557 primarily along the hydrological gradient (e.g. Andrus et al. 1986; Rydin, 1986). In a context
558 where substantial change in peatland hydrology is expected under a changing climate in northern
559 areas (e.g. longer snow-free season, lower summer water table and more frequent droughts),
560 there is a pressing need to understand how peatland plant communities could react and how
561 *Sphagnum* species could redistribute under habitat changes. In this work, we developed ~~the~~
562 Peatland Moss Simulator (PMS), a process-based stochastic model, to simulate the competition
563 between *S. magellanicum* and *S. fallax*, two key species representing dry (hummock) and wet
564 (lawn) habitats in a poor fen peatland. We empirically showed that these two species differed in
565 characteristics that likely affect their competitiveness ~~along a moisture gradient~~.

566 ~~The~~ Capitulum water retention for the lawn-preferring species (*S. fallax*) was weaker than that
567 for the hummock-preferring species (*S. magellanicum*). Compared to *S. magellanicum*, the
568 capitula of *S. fallax* held less water at saturation and water content decreased more rapidly with
569 dropping water potential. Hence, *S. fallax* would dry faster than *S. magellanicum* under the same
570 rate of water loss. Moreover, ~~the~~ water content in *S. fallax* capitula was less resistant to
571 evaporation. These differences indicated that it is harder for *S. fallax* capitula to buffer
572 evaporative ~~water loss of water~~ and thereby avoid or delay desiccation. Similar differences
573 between hummock and hollow species have been found ~~also~~ earlier (Titus & Wagner, 1984;
574 Rydin & McDonald, 1985). In addition, the net photosynthesis of *S. fallax* is more sensitive to
575 changes in capitulum water content than ~~*S. magellanicum*~~ *S. magellanicum*, as seen in ~~a~~ steeper
576 decline in photosynthesis with decreasing water content (Fig. B2C). Consequently, ~~the growth of~~
577 *S. fallax* is more likely to be ~~constrained-slowed down~~ by dry periods, when the capillary water
578 cannot fully compensate the evaporative loss (Robroek et al., 2007b) making it less competitive
579 in habitats prone to desiccation.

580 The PMS successfully captured the habitat preferences of the two *Sphagnum* species (Test 1):
581 starting from a mixed community with equal probabilities for both species, the lawn habitats
582 with shallower water table were eventually dominated by the typical lawn species *S. fallax*,
583 whereas hummock habitats, which were 15 cm higher than the lawn surface, were taken over by
584 *S. magellanicum*. The low final cover of *S. magellanicum* simulated in lawn habitats agreed well
585 with field observation from our study site, where *S. magellanicum* cover was less than 1% in
586 lawns (Kokkonen et al., 2019). On the other hand, *S. fallax* was outcompeted by *S.*
587 *magellanicum* in the hummock habitats. This result is consistent with previous findings that
588 hollow-preferring *Sphagna* are less likely to survive in hummock environments with greater
589 drought pressure (see Rydin 1985; Rydin et al. 2006; Johnson et al., 2015). The simulated annual
590 height increments of mosses also agreed well with the observed values for both habitat types. ~~As~~
591 ~~was the case in~~ Our simulation for lawn habitat ~~shows that~~ the looser stem structure of *S.*

592 *fallax*, allows it to allocate more of ~~the-its~~ produced biomass into height growth, and there~~by~~
593 overgrow *S. magellanicum*, ~~in which new biomass forms a -that allocates the produced biomass~~
594 ~~to form~~ compact stem, packed with thick fascicles. This ~~finding~~ indicates~~ed~~ that PMS can
595 capture key mechanisms in controlling the growth and ~~competitive~~ interactions of the *Sphagnum*
596 species.

597 ~~The testing of~~ parameter sensitivity ~~testing~~ showed the robustness of PMS regarding the
598 uncertainties in parameterization, as the simulated changes in the mean species cover, ~~under 10%~~
599 ~~changes in several parameters,~~ were generally less than the standard deviations of the means
600 ~~under 10% changes in several parameters.~~ We found that~~D~~ decreasing the value of ~~the~~ hydraulic
601 parameter n (Table 3, Eq. A5) increased the presence of *S. fallax* in the hummock habitats. This
602 was expected as n is a scaling factor and therefore its changes get magnified: a lower n value
603 will lead to higher water content in the unsaturated layers ~~above the water table~~ (van Genuchten,
604 1978), which ~~allows is important to~~ wet-adapted *Sphagna* ~~in order~~ to survive dry conditions
605 (Hayward and Clymo, 1982; Robroek et al., 2007b; Rice et al., 2008). In contrast, the response
606 of *Sphagnum* cover to the changes in other hydraulic parameters (i.e. α , n , K_h) ~~was~~ limited in
607 lawn habitats. This could be due to the relatively shallow water table in lawns, which was able to
608 maintain sufficient capillary rise to the moss carpet and capitula. Decreasing the values of ~~the~~
609 ~~specific immobilization rate (kimm-)~~ and ~~maximal NSC concentration in Sphagnum biomass~~
610 (NSC_{max}) mainly decreased the cover of *S. fallax* in lawn habitats, consistent with the importance
611 of biomass production to *Sphagna* in high moisture environment (e.g. Rice et al., 2008; Laine et
612 al., 2011). In addition, the SVAT modelling for hummocks and lawns (Module III, Fig. 1)
613 employed same hydraulic parameter values obtained from *S. magellanicum* hummocks
614 (McCarter and Price, 2014). ~~For lawns,~~ (This could overestimate K_m but underestimate n ~~for~~
615 ~~lawns,~~ as the lawn peat ~~would be~~ could be less efficient in ~~holding high~~ water ~~retention content~~
616 and ~~generating~~ capillary-flow ~~generation, as compared to~~ than hummock peat (Robroek et al.,
617 2007b; Branham and Strack, 2014). As the decrease in K_m and increase in n showed
618 counteracting effects on the simulated species covers (Table 4), the biases in the
619 parameterization of K_m and n may not critically impact model performance.

620 Both our empirical measurements and PMS simulations indicate the importance of capitulum
621 water ~~retention content-~~ as a mechanism controlling the moss community dynamics in peatlands.
622 It has long been hypothesized and experimentally studied that *Sphagnum* niche is defined by two
623 processes. Firstly, dry, high elevation habitats such as hummocks physically select species with
624 ability to remain moist (Rydin, 1993).— If the interspecific differences in water retention and
625 water-stress effects were correctly specified (Test 1, Fig. 2) our model predicted this phenomena
626 of stronger competitiveness of *S. magellanicum* against *S. fallax* in hummock habitats correctly.
627 Alternatively, the model failed to predict the distribution of *S. magellanicum* on hummocks, if
628 these interspecific differences ~~in the water processes~~ were neglected (Test 3 and Test 4, Fig. 3).
629 During low water table periods in summer ~~the~~ capillary rise may not fully compensate for ~~the~~

630 high evaporation (Robroek et al., 2007b; Nijp et al., 2014). In such circumstances, capitulum
631 water potential could drop rapidly towards the pressure defined by the relative humidity of air
632 (Hayward and Clymo, 1982). Consequently, the ability of capitula to retain cytoplasmic water
633 ~~would be~~ particularly important for the hummock-preferring species, as was also shown by
634 Titus & Wagner (1984).

635 Secondly, ~~r~~-in habitats with more persistently high moisture content such as lawns and
636 hollows, ~~the~~ interspecific competition becomes important: ~~it is well acknowledged that species~~
637 from such habitats generally have higher growth rates and photosynthetic capacity compared to
638 hummock species (e.g. Laing et al., 2014; Bengtsson et al., 2016). Our results also agreed on
639 this, as setting the growth-related parameters (i.e. Pm_{20} , RS_{20} , α_{PPFD} and H_{spec}) of *S. magellanicum*
640 to be the same as those of *S. fallax* decreased the *S. fallax* cover in both hummock and lawn
641 habitats (Test 6, Fig. 4B). However, ~~the model still captured the such changes didn't impact the~~
642 simulated habitat preferences for the tested species ~~without including the interspecific~~
643 ~~differences in those growth-related parameters~~. Based on this, the growth-related parameters
644 ~~could seem to~~ be less important than those water-related ones. Further on, our Tests 7 and 8
645 showed that when interspecific differences in the water-stress effects on photosynthesis were
646 removed, the model still predicted the correct habitat preferences of *S. magellanicum* and *S.*
647 *fallax*. Therefore, the interspecific differences in capitulum water retention could be the main
648 determinant on the habitat preferences of the tested species.

649

650 There have been growing concerns ~~on~~ about the shift of peatland communities from
651 *Sphagnum*-dominated towards more vascular-abundant under a drier and warmer climate
652 (Wullschleger et al., 2014; Munir et al. 2015; Dieleman et al. 2015). Nevertheless, the potential
653 of *Sphagnum* species composition to adjust to this forcing remains poorly understood.
654 Particularly in oligotrophic fens, where the vegetation is substantially shaped by lateral
655 hydrology (Tahvanainen, 2011; Turetsky et al., 2012), plant communities can be highly
656 vulnerable to hydrological changes (Gunnarsson et al. 2002; Tahvanainen, 2011). Based on the
657 validity and robustness of PMS, we believe PMS could serve as one of the first mechanistic tools
658 to investigate the direction and rate of change in *Sphagnum* communities ~~to change~~ under
659 environmental forcing. The hummock-lawn differences showed by Test 1 ~~implied~~ that *S.*
660 *magellanicum* could outcompete *S. fallax* within a decadal time frame in a poor fen community,
661 if the water table of habitats like lawns was lowered by 15 cm (Test 1). Although this was
662 derived from a simplified system with only the two species, it highlighted the potential of rapid
663 turnover of *Sphagnum* species: the hummock-lawn difference of water table in simulation was
664 comparable to the expected water table drawdown in fens under the warming climate
665 (Whittington and Price, 2006; Gong et al., 2013b). The effect traits of mosses, while studied less
666 than those of vascular plant traits, have far reaching impacts on biogeochemistry of ecosystems

667 such as peatlands, where mosses form the most significant plant group (Cornelissen et al. 2007).
668 Because of the large interspecific differences of traits such as photosynthetic potential, hydraulic
669 properties and litter chemistry (Laiho 2006; Straková et al., 2011; Korrensalo et al., 2017; Jassey
670 & Signarbieux, 2019), change in *Sphagnum* community composition is likely to impact long-
671 term peatland stability and functioning (Waddington et al., 2015). Turnover between hummock
672 and wetter habitat species would feedback to climate as they differ in their decomposability
673 (Straková et al. 2012; Bengtsson et al. 2016). As hummock species produces more calcitrant
674 litter the carbon bind into the system would take longer to get released back to atmosphere. In
675 addition, the replacement of wet adapted moss species with hummock species is likely to result
676 in higher ability to maintain carbon sink under periods of drought (Jassey, & Signarbieux, 2019).

677 Although efforts have been made on analytical modelling to obtain boundary conditions for
678 equilibrium states of moss and vascular communities in peatland ecosystems (Pastor et al.,
679 2002), the dynamical process of peatland vegetation has not been well-described or included in
680 earth system models (ESMs). Existing ecosystem models usually consider the features of
681 peatland moss cover as “fixed” (Sato et al., 2007; Wania et al., 2009; Euskirchen et al., 2014), or
682 change directionally following a projected trajectory (Wu and Roulet, 2014). [Chaudhury et al.](#)
683 [\(2017\) have a dynamic peatland vegetation model, with a single moss PFT and four vascular](#)
684 [PFTs, so moss productivity relative to vascular plants can vary, however moss characteristics are](#)
685 [fixed to a single set of values.](#) Our modelling approach provided a way to incorporate the
686 [environmental fluctuation and the](#) mechanisms of dynamical moss cover into peatland carbon
687 modelling. PMS employed an individual-based approach where each grid cell carries a unique
688 set of trait properties, so that shoots with favorable trait combinations in prevailing environment
689 are thus able to replace those whose trait combinations are less favorable. [Moreover, the model](#)
690 [included the spatial interactions of individuals, which can impact the sensitivity of coexistence](#)
691 [pattern to environmental changes \(Bolker et al., 2003; Sato et al., 2007; Tatsumi et al., 2019\).](#)
692 This mimics the stochasticity in plant responses to environmental fluctuations, which ~~are~~-is
693 essential to community assembly and trait filtering under environmental forcing (Clark et al.,
694 2010). [The importance of incorporating environmental fluctuations with the stochasticity of](#)
695 [biophysiological processes is supported by our Test 9 and 10. If the monthly mean climate](#)
696 [conditions were used as input, our model failed to predict the dominance of *S. magellanicum* on](#)
697 [hummocks. If the stochasticity of model parameters were omitted and only mean values were](#)
698 [used, the model generated only single output disregarding the randomness of environmental](#)
699 [conditions. Moreover, the model included the spatial interactions of individuals, which can](#)
700 [impact the sensitivity of coexistence pattern to environmental changes \(Bolker et al., 2003; Sato](#)
701 [et al., 2007; Tatsumi et al., 2019\).](#) Because ~~As~~ these features are [considered](#) essential to the
702 “next generation” DVMs (Scheiter et al., 2013), [our PMS with competition based on growth](#)
703 [rates](#) could be considered as an elemental design for future DVM development.

704 ~~To conclude, our PMS could successfully capture the habitat preferences of the modelled~~

705 *Sphagnum*. In this respect, our PMS model could provide fundamental support for the future
706 development of dynamic vegetation models for peatland ecosystems. Based on our findings, the
707 capitulum water processes should be considered as a control on the vegetation dynamics in future
708 impact studies on peatlands under changing environmental conditions.

709 We see PMS as an elemental design for the future development of dynamic vegetation models
710 for peatland ecosystems, yet there are certain uncertainties and features that should be developed
711 further. We used a gas-exchange-based method to quantify the simultaneous changes in capitula
712 water potential, water content and carbon uptake of *Sphagnum* moss capitula. It should be noted
713 that, the measurements mainly covered the changes from RWC_{opt} towards RWC_{cmp} (Table 1 and
714 Fig. 3). However, capitula water content could be higher than RWC_{opt} at saturation (e.g. about
715 25-30 g g⁻¹; Schipperges and Rydin, 1998). When RWC is high, vapor diffusion may occur
716 mainly from the capitula surface or macropores, instead of the inside capitula. Hence, our
717 methodology may not be suitable to reflect the water potential changes under near-saturation
718 conditions. In our modelling, we used the volumetric water content of moss carpet to estimate
719 RWC as an approximation for wet conditions (Eq. 17). The accuracy of such approximation for
720 high RWC conditions remains ambiguous and more information is still required.

721 We assumed that tissue structure did not change during the measurement process, and that the
722 aerodynamic resistance (r_a , Eq. 3) for vapor to diffuse from the inner capitula to the headspace
723 was constant. However, capitula drying may change leaf curvature, especially in species with
724 slim and sparsely spread leaves (Laine et al., 2018). Such changes in the branch-leaf structure
725 could expose the more of the leaf surface to evaporation and reduce the value of r_a .
726 Consequently, PMS could underestimate capitula water potential towards the drying end for
727 those species, if a constant r_a is derived from the maximal evaporation rate (E_m , Eq. 5; Fig 3C).

728 The water-retention relationship in PCM may not sufficiently capture water potential changes at
729 wet and dry extremes (e.g., *S. magellanicum* in Fig. 4C). Water retention functions developed
730 for mineral soils (e.g., Clapp and Hornberge, 1978; van Genuchten, 1980) may not be well
731 parameterized for peat soils and moss (non-vacular) vegetation, particularly under very dry or
732 wet conditions. Hence, further studies are needed to improve the description of the nonlinearity
733 of capitula water content, as influenced by capitula morphology (e.g. capitula biomass and shoot
734 density) and structural changes of branch leaves.

735 PMC lacks horizontal (lateral) water transport that may allow individuals of lawn species to be
736 present in hummocks (Rydin 1985). With additional experimental data, such as species-specific
737 hydraulic conductivity, the current model could be improved to also quantify the horizontal
738 water transport among neighboring grid cells.

739 To conclude, PMS could successfully capture the habitat preferences of the modelled *Sphagnum*
740 species. In this respect, PMS could provide fundamental support for the future development of
741 dynamic vegetation models for peatland ecosystems. Based on our findings, capitulum water

742 [processes should be considered as a control on vegetation dynamics in future impact studies on](#)
743 [peatlands under changing environmental conditions.](#)

744

745 **Acknowledgements**

746 We are grateful to Harri Strandman (University of Eastern Finland) for the coding of Weather
747 Generator. The project was funded by Academy of Finland (Project number 287039). AML
748 acknowledges support from the Kone Foundation and SF from grant #1802825 from the US
749 National Science Foundation, and the Fulbright-Finland and Saastamoinen Foundations.
750

751 *Code and data availability.* The data and the code to reproduce the analysis is available upon
752 request to the corresponding author.

753 *Author contributions.* JG and EST designed the study. JG, AML and NK conducted the
754 experiment and analysis. JG, EST, NR and SF designed the model. JG coded the model and
755 conducted the model simulation and data analysis. JG and EST wrote the manuscript with
756 contributions from all co-authors.

757 *Competing interests.* The authors declare that they have no conflict of interest.

758

759 **References**

760 Alm, J., Shurpali, N. J., Tuittila, E.-S., Laurila, T., Maljanen, M., Saarnio, S. and Minkkinen, K.:
761 Methods for determining emission factors for the use of peat and peatlands – flux measurements
762 and modelling, *Boreal Environment Research*, 12, 85-100, 2007.

763 Amarasekare, P.: Competitive coexistence in spatially structured environments: A synthesis,
764 *Ecology Letters*, 6, 1109-1122, 2003.

765 Anderson K. and Neuhauser C.: Patterns in spatial simulations—are they real? *Ecological*
766 *Modelling*, 155, 19-30, 2000.

767 Andrus R. E.: Some aspects of Sphagnum ecology, *Can. J. Bot.*, 64, 416–426, 1986.

768 Asaeda, T. and Karunaratne, S.: Dynamic modelling of the growth of Phragmites australis:
769 model description, *Aquatic Botany*, 67, 301-318, 2000.

770 Bengtsson, F., Granath, G. and Rydin, H.: Photosynthesis, growth, and decay traits in Sphagnum
771 - a multispecies comparison. *Ecology and Evolution*, 6, 3325-3341, 2016.

772 Blois, J. L., Williams, J. W., Fitzpatrick, M. C., Jackson, S. T. and Ferrier S.: Space can
773 substitute for time in predicting climate-change effects on biodiversity, *PNAS*, 110, 9374-9379,
774 doi:10.1073/pnas.1220228110, 2013.

775 Breeuwer, A., Heijmans, M. M., Robroek, B. J. ~~and~~ Berendse, F. ~~;(2008)~~. The effect of
776 temperature on growth and competition between Sphagnum species. *Oecologia*, 156(1), 155-67,
777 [2008](#).

778 Bolker, B. M., Pacala, S. W. and Neuhauser, C.: Spatial dynamics in model plant communities:
779 What do we really know? *Am. Nat.*, 162, 135–148, 2003.

780 Boulangeat, I., Svenning, J. C., Daufresne, T., Leblond, M. and Gravel, D.: The transient
781 response of ecosystems to climate change is amplified by trophic interactions, *Oikos*, 127, 1822–
782 1833, 2018.

783 Branham, J. E. and Strack, M.: Saturated hydraulic conductivity in *Sphagnum*-dominated
784 peatlands: do microforms matter? *Hydrol. Process.*, 28, 4352-4362, 2014.

785 [Chaudhary, N., Miller, P. A., and Smith, B. Modelling Holocene peatland dynamics with an](#)
786 [individual-based dynamic vegetation model. *Biogeosciences*, 14, 2571–2596, 2017.](#)

787 Chesson, P. ~~;(2000)~~: General theory of competitive coexistence in spatially varying
788 environments. *Theoretical Population Biology* 58, 211–237, [2000](#).

789 Clapp, R. B. ~~and~~ Hornberger, G. M. ~~;(1978)~~. Empirical equations for some soil hydraulic
790 properties. *Water Resour. Res.*, 14, 601–604, [1978](#).

791 Clark J. S., Bell D., Chu C., Courbaud B., Dietze M., Hersh M., HilleRisLambers J., Ibanez I.,
792 LaDeau S., McMahon S., Metcalf, J., Mohan, J., Moran, E., Pangle, L., Pearson, S., Salk, C.,
793 Shen, Z., Valle, D. and Wyckoff, P.: High-dimensional coexistence based on individual
794 variation: a synthesis of evidence, *Ecological Monographs*, 80, 569 – 608, 2010.

795 Clymo, R. S.: The growth of Sphagnum: Methods of measurement, *Journal of Ecology*, 58, 13-
796 49, 1970.

797 Cornelissen, J. H., Lang, S. I., Soudzilovskaia, N. A., and During, H. J.: Comparative cryptogam
798 ecology: a review of bryophyte and lichen traits that drive biogeochemistry. *Annals of botany*,
799 99(5), 987-1001, 2007

800

801 Czárán T. and Iwasa Y.: Spatiotemporal models of population and community dynamics, *Trends*
802 *Ecol. Evol.*, 13, 294–295, 1998.

803 Dieleman, C. M., Branfireun, B. A., Mclaughlin, J. W. and Lindo, Z.: Climate change drives a
804 shift in peatland ecosystem plant community: Implications for ecosystem function and stability,
805 *Global Change Biology*, 21, 388-395, 2015.

806 Euskirchen, E. S., Edgar, C. W., Turetsky, M. R., Waldrop, M. P. and Harden J. W.: Differential
807 response of carbon fluxes to climate in three peatland ecosystems that vary in the presence and
808 stability of permafrost, *J. Geophys. Res. Biogeosci.*, 119, 1576–1595, 2014.

809 Frohling, S., Roulet, N. T., Moore, T. R., Lafleur, T. M., Bubier, L. J. and Crill, P. M.: Modeling
810 seasonal to annual carbon balance of Mer Bleue Bog, Ontario, Canada. *Global Biogeochem.*
811 *Cycles*, 16, doi:10.1029/2001GB001457, 2002.

812 Gassmann, F., Klötzli, F. and Walther, G.: Simulation of observed types of dynamics of plants
813 and plant communities, *Journal of Vegetation Science*, 11, 397 – 408, 2003.

814 Goetz, J. D. and Price, J. S.: ~~(2015)~~ Role of morphological structure and layering of *Sphagnum*
815 and *Tomenthypnum* mosses on moss productivity and evaporation rates. *Canadian Journal of Soil*
816 *Science*, 95, 109-124, [2015](#).

817 Gong, J., Shurpali, N., Kellomäki, S., Wang, K., Salam, M. M. and Martikainen, P. J.: High
818 sensitivity of peat moisture content to seasonal climate in a cutaway peatland cultivated with a
819 perennial crop (*Phalaris arundinacea*, L.): a modeling study, *Agricultural and Forest*
820 *Meteorology*, 180, 225–235, 2013a.

821 Gong, J., Wang, K., Kellomäki, S., Wang, K., Zhang, C., Martikainen, P. J. and Shurpali, N.:
822 Modeling water table changes in boreal peatlands of Finland under changing climate conditions,
823 *Ecological Modelling*, 244, 65-78, 2013b.

824 Gong, J., Jia, X., Zha, T., Wang, B., Kellomäki, S. and Peltola, H.: Modeling the effects of plant-
825 interspace heterogeneity on water-energy balances in a semiarid ecosystem, *Agricultural and*
826 *Forest Meteorology*, 221, 189–206, 2016.

827 Gorham, E.: Northern peatlands: Role in the carbon cycle and probable responses to climatic
828 warming, *Ecol. Appl.*, 1, 182–195, 1991.

829 Gunnarsson, U., Malmer, N. and Rydin, H.: Dynamics or constancy in *Sphagnum* dominated
830 mire ecosystems? A 40-year study, *Ecography*, 25, 685–704, 2002.

831 Hartmann, H. and Trumbore, S.: Understanding the roles of nonstructural carbohydrates in forest
832 trees – from what we can measure to what we want to know, *New Phytol.*, 211, 386-403, 2016.

833 Hájek, T. and Beckett, R. P.: Effect of water content components on desiccation and recovery in
834 *Sphagnum* mosses, *Annals of Botany*, 101, 165–173, 2008.

835 Hájek, T., Tuittila, E.-S., Ilomets, M. and Laiho, R.: Light responses of mire mosses - A key to
836 survival after water-level drawdown? *Oikos*, 118, 240-250, 2009.

837 Hayward P. M. and Clymo R. S.: Profiles of water content and pore size in *Sphagnum* and peat,
838 and their relation to peat bog ecology. *Proceedings of the Royal Society of London, Series B,*
839 *Biological Sciences*, 215, 299-325, 1982.

840 Hayward P. M. and Clymo R. S.: The growth of *Sphagnum*: experiments on, and simulation of,
841 some effects of light flux and water-table depth. *Journal of Ecology*, 71, 845-863, 1983.

842 Holmgren, M., Lin, C., Murillo, J. E., Nieuwenhuis, A., Penninkhof, J., Sanders, N., Bart, T.,

843 Veen, H., Vasander, H., Vollebregt, M. E. and Limpens, J.: Positive shrub–tree interactions
844 facilitate woody encroachment in boreal peatlands, *J. Ecol.*, 103, 58-66, 2015.

845 Hugelius, G., Tarnocai, C., Broll, G., Canadell, J. G., Kuhry, P. and Swanson, D. K.: The
846 Northern Circumpolar Soil Carbon Database: spatially distributed datasets of soil coverage and
847 soil carbon storage in the northern permafrost regions, *Earth Syst. Sci. Data*, 5, 3-13, 2013.

848 Jassey, V. E., & Signarbieux, C.: Effects of climate warming on Sphagnum photosynthesis in
849 peatlands depend on peat moisture and species-specific anatomical traits. *Global change biology*,
850 25(11), 3859-3870, 2019.

851 Johnson, M. G., Granath, G., Tahvanainen, T., Pouliot, R., Stenøien, H. K., Rochefort, L., Rydin,
852 H. and Shaw, A. J.: Evolution of niche preference in Sphagnum peat mosses, *Evolution*, 69, 90 –
853 103, 2015.

854 Kellomäki, S. and Väisänen, H.: Modelling the dynamics of the forest ecosystem for climate
855 change studies in the boreal conditions, *Ecol. Model.*, 97, 121-140, 1997.

856 Keuper, F., Dorrepaal, E., Van Bodegom, P. M., Aerts, R., Van Logtestijn, R. S.P., Callaghan, T.
857 V. and Cornelissen, J. H.C.: A Race for Space? How Sphagnum fuscum stabilizes vegetation
858 composition during long-term climate manipulations, *Global Change Biology*, 17, 2162–2171,
859 2011.

860 Kokkonen, N., Laine, A., Laine, J., Vasander, H., Kurki, K., Gong, J. and Tuittila, E.-S.:
861 Responses of peatland vegetation to 15-year water level drawdown as mediated by fertility level.
862 *J. Veg. Sci.*, 30(6), 1206-1216, 2019.

863 Korrensalo, A., Hájek, T., Vesala, T., Mehtätalo, L., ~~and~~ Tuittila, E. S.: ~~(2016)~~. Variation in
864 photosynthetic properties among bog plants. *Botany*, 94(12), 1127-1139, [2016](#).

865 Korrensalo, A., Alekseychik, P., Hájek, T., Rinne, J., Vesala, T., Mehtätalo, L., Mammarella, I.
866 and Tuittila, E.-S.: Species-specific temporal variation in photosynthesis as a moderator of
867 peatland carbon sequestration, *Biogeosciences*, 14, 257-269, 2017.

868 Kyrkjeide, M. O., Hassel, K., Flatberg, K. I., Shaw, A. J., Yousefi, N. and Stenøien, H. K.
869 Spatial genetic structure of the abundant and widespread peatmoss Sphagnum magellanicum
870 *Brid. PLoS One*, 11, e0148447, 2016.

871 Laiho, R. Decomposition in peatlands: Reconciling seemingly contrasting results on the impacts
872 of lowered water levels, *Soil Biology and Biochemistry*, 38, 2011-2024, 2006.

873 Laine, A. M. Juurola, E., Hájek, T., [and](#) Tuittila, E.-S.: ~~(2011)~~. Sphagnum growth and
874 ecophysiology during mire succession. *Oecologia*, 167: 1115-1125, [2011](#).

875 Laine, J., Komulainen, V.-M., Laiho, R., Minkkinen, K., Ras-
876 Sarkkola, S., Silvan, N., Tolonen, K., Tuittila, E.-S., Vasander, H., and Päivänen, J.: ~~(2004)~~.

877 Lakkasuo – a guide to mire ecosystem, Department of Forest Ecology Publications, University of
878 Helsinki, 31, 123 pp, [2004](#).

879 Laine, J., Flatberg, K. I., Harju, P., Timonen, T., Minkkinen, K., Laine, A., Tuittila, E.-S. ~~and~~
880 Vasander, H. ~~(2018)~~; Sphagnum Mosses — The Stars of European Mires. University of Helsinki
881 Department of Forest Sciences, Sphagna Ky. 326 p, [2018](#).

882 Laine J., Harju P., Timonen T., Laine A., Tuittila E.-S., Minkkinen K. and Vasander H.: The
883 intricate beauty of Sphagnum mosses—a Finnish guide to identification (Univ Helsinki Dept
884 Forest Ecol Publ 39). Department of Forest Ecology, University of Helsinki, Helsinki, pp 1–190,
885 2009.

886 Laing, C. G., Granath, G., Belyea, L. R., Allton K. E. and Rydin, H.: Tradeoffs and scaling of
887 functional traits in Sphagnum as drivers of carbon cycling in peatlands, *Oikos*, 123, 817–828,
888 2014.

889 Larcher, W.: *Physiological Plant Ecology: Ecophysiology and Stress Physiology of Functional*
890 *Groups*, Springer, 2003.

891 Letts, M. G., Roulet, N. T. and Comer, N. T.: Parametrization of peatland hydraulic properties
892 for the Canadian land surface scheme, *Atmosphere-Ocean*, 38, 141-160, 2000.

893 Martínez-Vilalta, J., Sala, A., Asensio, D., Galiano, L., Hoch, G., Palacio, S., Piper, F. I. and
894 Lloret, F.: Dynamics of non-structural carbohydrates in terrestrial plants: a global synthesis. *Ecol*
895 *Monogr*, 86, 495-516, 2016.

896 McCarter C. P. R. and Price J. S.: Ecohydrology of Sphagnum moss hummocks: mechanisms of
897 capitula water supply and simulated effects of evaporation. *Ecohydrology* 7, 33 – 44, 2014.

898 Munir, T. M., Perkins, M., Kaing, E. and Strack, M.: Carbon dioxide flux and net primary
899 production of a boreal treed bog: Responses to warming and water-table-lowering simulations of
900 climate change, *Biogeosciences*, 12, 1091–1111, 2015.

901 Murray, K. J., Harley, P. C., Beyers, J., Walz, H. and Tenhunen, J. D.: Water content effects on
902 photosynthetic response of Sphagnum mosses from the foothills of the Philip Smith Mountains,
903 Alaska, *Oecologia*, 79, 244-250, 1989.

904 Nijp, J. J., Limpens, J., Metselaar, K., van der Zee, S. E. A. T. M., Berendse, F. and Robroek B.
905 J. M.: Can frequent precipitation moderate the impact of drought on peatmoss carbon uptake in
906 northern peatlands? *New Phytologist*, 203, 70-80, 2014.

907 O’Neill, K. P.: Role of bryophyte-dominated ecosystems in the global carbon budget. In A. J.
908 Shaw and B. Goffi net [eds.] *Bryophyte biology*, 344–368, Cambridge University Press,
909 Cambridge, UK, 2000.

910 Pastor, J., Peckham, B., Bridgham, S., Weltzin, J. and Chen J.: Plant community dynamics,

911 nutrient cycling, and alternative stable equilibria in peatlands. *American Naturalist*, 160, 553-
912 568, 2002.

913 Päivänen, J.: Hydraulic conductivity and water retention in peat soils, *Acta Forestalia Fennica*,
914 129, 1-69, 1973.

915 Pouliot, R., Rochefort, L., Karofeld, E. [and](#); Mercier, C.: ~~(2011)~~ Initiation of *Sphagnum* moss
916 hummocks in bogs and the presence of vascular plants: Is there a link? *Acta Oecologica*, 37, 346-
917 354, [2011](#).

918 Price, J. S., Whittington, P. N., Elrick, D. E., Strack, M., Brunet, N. and Faux, E.: A method to
919 determine unsaturated hydraulic conductivity in living and undecomposed moss, *Soil Sci. Soc.*
920 *Am. J.*, 72, 487 – 491, 2008.

921 Price, J. S. and Whittington, P. N.: Water flow in *Sphagnum* hummocks: Mesocosm
922 measurements and modelling, *Journal of Hydrology* 381, 333 – 340, 2010.

923 Rice, S. K., Aclander, L. and Hanson, D. T.: Do bryophyte shoot systems function like vascular
924 plant leaves or canopies? Functional trait relationships in *Sphagnum* mosses (Sphagnaceae),
925 *American Journal of Botany*, 95, 1366-1374, 2008.

926 Riutta, T., Laine, J., Aurela, M., Rinne, J., Vesala, T., Laurila, T., Haapanala, S., Pihlatie, M. and
927 Tuittila, E.-S.: Spatial variation in plant community functions regulates carbon gas dynamics in a
928 boreal fen ecosystem, *Tellus*, 59B, 838-852, 2007.

929 Robroek, B. J.M., Limpens, J., Breeuwer, A., Crushell, P. H. and Schouten, M. G.C.:
930 Interspecific competition between *Sphagnum* mosses at different water tables, *Functional*
931 *Ecology*, 21, 805 – 812, 2007a.

932 Robroek, B. J.M., Limpens, J., Breeuwer, A., van Ruijven, J. and Schouten, M. G.C.:
933 Precipitation determines the persistence of hollow *Sphagnum* species on hummocks, *Wetlands*,
934 4, 979 – 986, 2007b.

935 Robroek, B. J.M., Schouten, M. G.C., Limpens, J., Berendse, F. and Poorter, H.: Interactive
936 effects of water table and precipitation on net CO₂ assimilation of three co-occurring *Sphagnum*
937 mosses differing in distribution above the water table, *Global Change Biology* 15, 680 – 691,
938 2009.

939 Ruder, S.: An overview of gradient descent optimization algorithms, CoRR, abs/1609.04747,
940 2016.

941 Runkle, B.R.K., Wille, C., Gažovič M., Wilmking, M. and Kutzbach, L.: The surface energy
942 balance and its drivers in a boreal peatland fen of northwestern Russia, *Journal of Hydrology*,
943 511, 359-373, 2014.

944 Rydin, H: Interspecific competition between *Sphagnum* mosses on a raised bog. *Oikos*, 413-423,

945 1993.

946 Rydin, H.: Competition and niche separation in Sphagnum. Canadian Journal of Botany, 64(8),
947 1817-1824, 1986.

948 Rydin, H.: Competition between Sphagnum species under controlled conditions. Bryologist, 302-
949 307, 1997. Rydin, H. and McDonald A. J. S.: Tolerance of Sphagnum to water level. Journal of
950 Bryology, 13, 571-578, 1985.

951 Rydin, H., Gunnarsson, U., and Sundberg, S.: The role of Sphagnum in peatland development
952 and persistence, in: Boreal peatland ecosystems, edited by: Wieder, R. K., and Vitt, D. H., 30
953 Ecological Studies Series, Springer Verlag, Berlin, 47-65, 2006.

954 Sato, H., Itoh, A. and Kohyama, T.: SEIB-DGVM: A new Dynamic Global Vegetation Model
955 using a spatially explicit individual-based approach, Ecol. Model., 200, 279-307, 2007.

956 Scheiter, S., Langan, L. and Higgins, S. I.: Next-generation dynamic global vegetation models:
957 learning from community ecology, New Phytologist, 198, 957-969, 2013.

958 Schipperges, B. and Rydin, H.: Response of photosynthesis of Sphagnum species from
959 contrasting microhabitats to tissue water content and repeated desiccation, The New Phytologist,
960 140, 677-684, 1998.

961 Silvola, J., Aaltonen, H.: ~~(1984)~~ Water content and photo- synthesis in the peat mosses
962 Sphagnum fuscum and S. angustifolium. Annales Botanici Fennici 21, 1-6, [1984](#).

963 Smirnov, N.: The carbohydrates of bryophytes in relation to desiccation tolerance, Journal of
964 Bryology, 17, 185-19, 1992.

965 Straková, P., Niemi, R. M., Freeman, C., Peltoniemi, K., Toberman, H., Heiskanen, I., Fritze, H.
966 and Laiho, R.: Litter type affects the activity of aerobic decomposers in a boreal peatland more
967 than site nutrient and water table regimes, Biogeosciences, 8, 2741-2755, 2011.

968 Straková, P., Penttilä, T., Laine, J., and Laiho, R.: Disentangling direct and indirect effects of
969 water table drawdown on above-and belowground plant litter decomposition: consequences for
970 accumulation of organic matter in boreal peatlands. Global Change Biology, 18, 322-335, 2012.

971 Strandman, H., Väisänen, H. and Kellomäki, S.: A procedure for generating synthetic weather
972 records in conjunction of climatic scenario for modelling of ecological impacts of changing
973 climate in boreal conditions, Ecol. Model., 70, 195-220, 1993.

974 Szurdoki, E., Márton, O., Szövényi, P.: Genetic and morphological diversity of *Sphagnum*
975 *angustifolium*, *S. flexuosum* and *S. fallax* in Europe. Taxon, 63, 237-48, 2014.

976 Tahvanainen, T.: Abrupt ombrotrophication of a boreal aapa mire triggered by hydrological
977 disturbance in the catchment, Journal of Ecology, 99, 404-415, 2011.

978 Tatsumi, S., Cadotte M. W. and Mori, A. S.: Individual-based models of community assembly:

979 Neighbourhood competition drives phylogenetic community structure, *J. Ecol.*, 107, 735–746,
980 2019.

981 Thompson, D. K., Baisley, A. S. and Waddington, J. M.: Seasonal variation in albedo and
982 radiation exchange between a burned and unburned forested peatland: implications for peatland
983 evaporation, *Hydrological Processes*, 29, 3227–3235, 2015.

984 Titus, J. E., and Wagner, D. J.: Carbon balance for two *Sphagnum* mosses: water balance
985 resolves a physiological paradox. *Ecology*, 65(6), 1765–1774, 1984.
986

987 Turetsky, M. R.: The role of bryophytes in carbon and nitrogen cycling, *Bryologist*, 106, 395 –
988 409, 2003.

989 Turetsky, M. R., Crow, S. E., Evans, R. J., Vitt, D. H. and Wieder, R. K.: Trade-offs in resource
990 allocation among moss species control decomposition in boreal peatlands, *Journal of Ecology*,
991 96, 1297–1305, 2008.

992 Turetsky, M. R., Bond-Lamberty, B., Euskirchen, E., Talbot, J., Froking, S., McGuire, A. D.
993 and Tuittila, E.: The resilience and functional role of moss in boreal and arctic ecosystems, *New*
994 *Phytologist*, 196, 49–67, 2012.

995 van Gaalen, K. E., Flanagan, L. B., Peddle, D. R.: Photosynthesis, chlorophyll fluorescence and
996 spectral reflectance in *Sphagnum* moss at varying water contents. *Oecologia*, 153, 19 – 28, 2007.

997 van Genuchten, M.: A closed-form equation for predicting the hydraulic conductivity of
998 unsaturated soils, *Soil Science Society of American Journal*, 44, 892–898, 1980.

999 Välranta, M., Korhola, A., Seppä, H., Tuittila, E. S., Sarmaja-Korjonen, K., Laine, J. and Alm,
1000 J.: High-resolution reconstruction of wetness dynamics in a southern boreal raised bog, Finland,
1001 during the late Holocene: a quantitative approach, *The Holocene*, 17, 1093–1107, 2007.

1002 Venäläinen, A., Tuomenvirta, H., Lahtinen, R. and Heikinheimo, M.: The influence of climate
1003 warming on soil frost on snow-free surfaces in Finland, *Climate Change*, 50, 111–128, 2001.

1004 Vionnet, V., Brun, E., Morin, S., Boone, A., Faroux, S., Le Moigne, P., Martin, E. and Willemet,
1005 J.-M.: The detailed snowpack scheme Crocus and its implementation in SURFEX v7.2,
1006 *Geoscientific Model Development*, 5, 773–791, 2012

1007 Vitt, D. H.: Peatlands: Ecosystems dominated by bryophytes. In A. J. Shaw and B. Goffi net
1008 [eds.], *Bryophyte biology*, 312 – 343, Cambridge University Press, Cambridge, UK, 2000.

1009 Waddington, J. M., Morris, P. J., Kettridge, N., Granath, G., Thompson, D. K. and Moore, P. A.:
1010 Hydrological feedbacks in northern peatlands, *Ecohydrology*, 8, 113 – 127, 2015.

1011 Wania, R., Ross, I. and Prentice, I. C.: Integrating peatlands and permafrost into a dynamic
1012 global vegetation model: 2. Evaluation and sensitivity of vegetation and carbon cycle processes,
1013 *Global Biogeochemical Cycles*, 23, GB3015, DOI:10.1029/2008GB003413, 2009.

1014 Weiss, R., Alm, J., Laiho, R. and Laine, J.: Modeling moisture retention in peat soils, Soil
1015 Science Society of America Journal, 62, 305–313, 1998.

1016 Whittington, P. N. and Price, J. S.: The effects of water table draw-down (as a surrogate for
1017 climate change) on the hydrology of a fen peatland, Canada, Hydrological Processes, 20, 3589–
1018 3600, 2006.

1019 Wilson, P. G.: The relationship among micro-topographic variation, water table depth and
1020 biogeochemistry in an ombrotrophic bog, Master Thesis, Department of Geography McGill
1021 University, Montreal, Quebec, p. 103, 2012.

1022 Wojtuń B., Sendyk A. and Martynia, D.: Sphagnum species along environmental gradients in
1023 mires of the Sudety Mountains (SW Poland), Boreal Environment Research, 18, 74–88, 2003.

1024 Wu, J. and Roulet, N. T.: Climate change reduces the capacity of northern peatlands to absorb
1025 the atmospheric carbon dioxide: The different responses of bogs and fens. Global
1026 Biogeochemical Cycles, doi.org/10.1002/2014GB004845, 2014.

1027 Wullschleger, S. D., Epstein, H. E., Box, E. O., Euskirchen, E. S., Goswami, S., Iversen, C. M.,
1028 Kattge, J., Norby, R. J., van Bodegom, P. M. and Xu, X.: Plant functional types in Earth system
1029 models: past experiences and future directions for application of dynamic vegetation models in
1030 high-latitude ecosystems, Ann. Bot., 114, 1–16, 2014.

1031

1032 Table. 1 List of symbols and abbreviations

Symbol	Description	Unit
A	Net photosynthesis rate	$\mu\text{mol m}^{-2} \text{s}^{-1}$
A_m	Maximal net photosynthesis rate	$\mu\text{mol m}^{-2} \text{s}^{-1}$
α_{imm}	Temperature constant for NSC immobilization	
α_{PPFD}	Half-saturation point of PPFD for photosynthesis.	$\mu\text{mol m}^{-2} \text{s}^{-1}$
B_{cap}	Capitulum biomass	g m^{-2}
C_T	Specific heat	$\text{J K}^{-1} \text{kg}^{-1}$
D_S	Capitulum density	shoots cm^{-2}
dH	Annual height growth of <i>Sphagnum</i> mosses	cm
dWT	Hummock-lawn differences in water table	cm
E	Rate of evaporation	cm timestep ⁻¹
f_w	Water content multiplier on photosynthesis rate	
f_T	Temperature multiplier on photosynthesis rate	
h	Water potential	cm
H_c	Shoot height of <i>Sphagnum</i> mosses	cm
H_{cap}	Height of capitula	cm
H_{spc}	Biomass density of living <i>Sphagnum</i> stems	$\text{g m}^{-2} \text{cm}^{-1}$
I	Rate of net inflow water	cm
k_{imm}	Specific immobilization rate	g g^{-1}
JD_{thaw}	Julian day when thawing completed	
K_h	Hydraulic conductivity of peat layer	cm s^{-1}
K_m	Hydraulic conductivity of moss layer	cm s^{-1}

K_{sat}	Saturated hydraulic conductivity	cm s^{-1}
K_T	Thermal conductivity	$\text{W m}^{-1} \text{K}^{-1}$
lc	Width of a grid cell in simulation	cm
M_B	Immobilized NSC to biomass production	g
NSC_{max}	Maximal NSC concentration in <i>Sphagnum</i> biomass	g g^{-1}
P	Precipitation	cm
Pm	Mass-based rate of maximal gross photosynthesis	$\mu\text{mol g}^{-1} \text{s}^{-1}$
$PPFD$	Photosynthetic photon flux density	$\mu\text{mol m}^{-2} \text{s}^{-1}$
ρ_{bulk}	Bulk density of peat	g cm^{-3}
r_{aero}	Aerodynamic resistance	s m^{-1}
r_{bulk}	Cell-level bulk surface resistance	s m^{-1}
r_{ss}	Bulk surface resistance of community	s m^{-1}
Rh	Relative humidity	%
Rs	Mass-based respiration rate	$\mu\text{mol g}^{-1} \text{s}^{-1}$
R_s	Incoming shortwave radiation	W m^{-2}
R_l	Incoming longwave radiation	W m^{-2}
S_c	Area of a cell in model simulation	m^2
s_{imm}	Multiplier for temperature threshold	
Sv_i	Evaporative area of a cell i	cm^2
T	Capitulum temperature	$^{\circ}\text{C}$
Ta	Air temperature	$^{\circ}\text{C}$
T_{opt}	reference temperature of respiration (20 $^{\circ}\text{C}$)	$^{\circ}\text{C}$
u	Wind speed	m s^{-1}

W_{cap}	Capitulum water content	g g^{-1}
W_{cmp}	Capitulum water content at the compensation point	g g^{-1}
W_{max}	Maximum water content of capitula	g g^{-1}
W_{opt}	Optimal capitulum water content for photosynthesis	g g^{-1}
W_{cf}	field-water contents of <i>Sphagnum</i> capitulum	g g^{-1}
W_{sf}	field-water contents of <i>Sphagnum</i> stem	g g^{-1}
WTm	Measured multi-year mean of weekly water table	cm
WTs	Simulated multi-year mean of weekly water table	cm
z_m	Thickness of the living moss layer	cm
θ_m	Volumetric water content of moss layer	
θ_r	permanent wilting point water content	
θ_s	saturated water content	

Abbreviations:

Γ	Learning rate of gradient descent algorithms
D-layer	Daily-based snow layer
ICOS	Integrated Carbon Observation System
JD	Julian day
NSC	Nonstructural carbon
PMS	Peatland Moss Simulator
RWC	Capitulum water content
SD	Standard deviation
SE	Standard error
SSE	Sum of squared error

SVAT Soil-vegetation-atmosphere transport

WT Water table

1033
1034

1035 Table. 2 Species-specific values of morphological and photosynthetic parameters for *S.*
 1036 *magellanicum* and *S. fallax*. The parameters include: capitulum density (D_S), capitulum biomass
 1037 (B_{cap}), specific height of stem (H_{spc}), maximal gross photosynthesis rate at 20 °C (Pm_{20}),
 1038 respiration rate at 20 °C (Rs_{20}), half-saturation point of photosynthesis (α_{PPFD}), and polynomial
 1039 coefficients (a_{w0} , a_{w1} and a_{w2}) for the responses of net photosynthesis to capitulum water
 1040 content. Parameter values are given as mean \pm standard deviation.
 1041

Parameter	Unit	<i>S. magellanicum</i>	<i>S. fallax</i>	Equation
D_S	cm ²	0.922 \pm 0.289	1.46 \pm 0.323	- ^a
B_{cap}	g m ⁻²	75.4 \pm 21.5	69.2 \pm 19.6	- ^a
H_{spc}	g ⁻¹ cm ⁻¹	45.4 \pm 7.64	32.6 \pm 6.97	(7)
Pm_{20}	μ mol g ⁻¹ s ⁻¹	0.0189 \pm 0.00420	0.0140 \pm 0.00212	(2)
Rs_{20}	μ mol g ⁻¹ s ⁻¹	0.00729 \pm 0.00352	0.00651 \pm 0.00236	(2)
α_{PPFD}	μ mol m ⁻² s ⁻¹	101.4 \pm 14.1	143 \pm 51.2	(2)
a_{w0}	unitless	-1.354 \pm 0.623	-1.046 \pm 0.129	(4)
a_{w1}	unitless	0.431 \pm 0.197	0.755 \pm 0.128	(4)
a_{w2}	unitless	-0.0194 \pm 0.0119	-0.0751 \pm 0.0223	(4)

1042 ^a the parameter was used in the linear models predicting the log₁₀-transformed capitulum water
 1043 potential (h) and bulk resistance (r_{bulk}) for *S. fallax* and *S. magellanicum*. The capitulum density
 1044 and photosynthetic parameter values measured here are well within the range of those reported in
 1045 literature for these species (McCarter & Price, 2014; Laing et al. 2014; Bengtsson et al. 2016;
 1046 Korrensalo et al. 2016).

1047 Table 3. Parameters values for SVAT simulations (Module III). The parameters include:
 1048 saturated hydraulic conductivity (K_{sat}), water retention parameters of water retention curves (α
 1049 and n), saturated water content (θ_s), permanent wilting point water content (θ_r), snow layer
 1050 surface albedos (a_s , a_i), the thermal conductivity (K_T), specific heat (C_T), maximal nonstructural
 1051 carbon (NSC) concentration (NSC_{max}).

Parameter	Value	Equation	Source
K_{sat}	162	A6	McCarter and Price, 2014
n	1.43	A5	McCarter and Price, 2014
α	2.66	A5	McCarter and Price, 2014
θ_s	0.95 ^a	A5	Päivänen, 1973
θ_r	0.071 ^b	A5	Weiss et al., 1998
a_s	0.15	A9	Runkle et al., 2014
a_i	0.02	A10	Thompson et al., 2015
$K_{T,water}$	0.57	A4	Letts et al., 2000
$K_{T,ice}$	2.20	A4	Letts et al., 2000
$K_{T,org}$	0.25	A4	Letts et al., 2000
$C_{T,water}$	4.18	A3	Letts et al., 2000
$C_{T,ice}$	2.10	A3	Letts et al., 2000
$C_{T,org}$	1.92	A3	Letts et al., 2000
NSC_{max}	0.045	6	Turetsky et al., 2008

1052 ^a The value was calculated from bulk density (ρ_{bulk}) as $\theta_s = 97.95 - 79.72\rho_{bulk}$ following Päivänen
 1053 (1973); ^b The value was calculated as $\theta_r = 4.3 + 67\rho_{bulk}$ following Weiss et al. (1998).

1054 Table 4. Results from the Test 2 addressing the robustness of the model to the uncertainties in a
 1055 set of parameters. Each parameter was increased or decreased by 10%. Model was run for *S.*
 1056 *magellanicum* and *S. fallax* in their preferential habitats. Difference in mean cover between
 1057 simulations under changed and unchanged parameter values are given with the standard
 1058 deviations (SD) of the means in brackets. The parameters include: specific immobilization rate
 1059 (*kimm*), maximal nonstructural carbon (NSC) concentration (*NSC_{max}*), hydraulic conductivity of
 1060 moss layer (*K_m*), hydraulic conductivity of peat layer (*K_h*), water retention parameters of water
 1061 retention curves (α and *n*), snow layer surface albedo (*a_s*) and aerodynamic resistance (*r_{aero}*).

Change in parameter value	Equation	Changes in simulated cover, % (SD)	
		<i>S. magellanicum</i> (hummock)	<i>S. fallax</i> (lawn)
<i>kimm</i> +10%	5	-1.2 (3.5)	-3.5 (3.8)
<i>kimm</i> -10%		+2.7 (0.4)	-5.0 (3.4)
<i>NSC_{max}</i> +10%	6	+4.5 (2.9)	+0.7 (3.0)
<i>NSC_{max}</i> -10%		-0.7 (4.0)	-4.8 (4.5)
<i>K_m</i> +10%	10	+1.0 (3.1)	-1.7 (2.3)
<i>K_m</i> -10%		-1.7 (2.7)	+4.1 (4.3)
<i>K_h</i> +10%	A1	-1.1 (3.0)	+1.1 (2.0)
<i>K_h</i> -10%		-1.8 (3.1)	-0.5 (2.7)
<i>n</i> +10%	A5	-1.6 (3.2)	-3.2 (3.2)
<i>n</i> -10%		-9.4 (3.6)	-0.3 (2.9)
α +10 %	A5	-0.5 (2.9)	-0.3 (2.3)
α -10 %		-1.3 (3.6)	+3.2 (1.0)
<i>a_s</i> +10%	A9	-2.2 (3.8)	+0.6 (2.1)
<i>a_s</i> -10%		+3.3 (3.4)	+1.2 (1.8)
<i>r_{aero}</i> +10%	A14, A15	-2.1 (3.4)	+0.3 (2.1)
<i>r_{aero}</i> -10%		-3.8 (4.4)	+2.3 (1.1)

062 [Table 5. Result from the Test 7-10 addressing the importance of meteorological fluctuations,](#)
 063 [stochasticity of model parameters and the photosynthetic water-response. In Test 7, monthly](#)
 064 [mean values of meteorological variables were used to drive the model simulation. In Test 8, the](#)
 065 [stochasticity of model parameters was removed, and average values were used to parameters at](#)
 066 [grid cell level. In Test 9-10, the photosynthetic water-response parameters \(i.e. \$a_{w0}\$, \$a_{w1}\$ and \$a_{w2}\$.](#)
 067 [See Table 2\) were set to be the same as those in *S. magellanicum* \(Test 9\) and same as those in *S.*](#)
 068 [fallax \(Test 10\). The mean cover of *S. magellanicum* on hummocks and *S. fallax* on lawns after](#)
 069 [the simulation of 15 year periods are listed in the table.](#)

Test	<i>S. magellanicum</i> (hummock)	<i>S. fallax</i> (lawn)
<u>7</u>	<u>73%</u>	<u>26%</u>
<u>8</u>	<u>90%</u>	<u>72%</u>
<u>9</u>	<u>14 %</u>	<u>100 %</u>
<u>10</u>	<u>100 %</u>	<u>100 %</u>

071
072

1073 **Appendix A. Calculating community SVAT scheme (Module III)**

1074 *Transport of water and heat in peat profile*

1075 Simulating the transport of water and heat in the peat profiles was based on Gong et al. (2012,
1076 2013). Here we list the key algorithms and parameters. Ordinary differential equations governing
1077 the vertical transport of water and heat in peat profiles were given as:

1078
$$C_h \frac{\partial h}{\partial t} = \frac{\partial}{\partial z} \left[K_h \left(\frac{\partial h}{\partial z} + 1 \right) \right] + S_h$$

1079 (A1)

1080
$$C_T \frac{\partial T}{\partial t} = \frac{\partial}{\partial z} \left(K_T \frac{\partial T}{\partial z} \right) + S_T$$
 (A2)

1081 where t is the time step; z is the thickness of peat layer; h is the water potential; T is the
1082 temperature; C_h and C_T are the specific capacity of water (i.e. $\partial\theta/\partial h$) and heat; K_h and K_T are the
1083 hydraulic conductivity and thermal conductivity, respectively; and S_h and S_T are the sink terms
1084 for water and energy, respectively.

1085 C_T and K_T were calculated as the volume-weighted sums from components of water, ice and
1086 organic matter:

1087
$$C_T = C_{water}\theta_{water} + C_{ice}\theta_{ice} + C_{org}(1 - \theta_{water} - \theta_{ice})$$

1088 (A3)

1089
$$K_T = K_{water}\theta_{water} + K_{ice}\theta_{ice} + K_{org}(1 - \theta_{water} - \theta_{ice})$$
 (A4)

1090 where C_{water} , C_{ice} and C_{org} are the specific heats of water, ice and organic matter, respectively;
1091 K_{water} , K_{ice} and K_{org} are the thermal conductivities of water, ice and organic matter, respectively;
1092 and θ_{water} and θ_{ice} are the volumetric contents of water and ice, respectively.

1093 For a given h , $C_h = \partial\theta(h)/\partial h$ was derived from the van Genuchten water retention model (van
1094 Genuchten, 1980) as:

1095
$$\theta(h) = \theta_r + \frac{(\theta_s - \theta_r)}{[1 + (\alpha|h^n|)^m]}$$
 (A5)

1096 where θ_s is the saturated water content; θ_r is the permanent wilting point water content; α is a
1097 scale parameter inversely proportional to mean pore diameter; n is a shape parameter; and $m = 1 -$
1098 $1/n$.

1099 Hydraulic conductivity (K_h) in an unsaturated peat layer was calculated as a function of θ by
1100 combining the van Genuchten model with the Mualem model (Mualem, 1976):

1101
$$K_h(\theta) = K_{sat} S_e^{L_e} \left[1 - \left(1 - S_e^{1/m} \right)^m \right]$$

1102 (A6)

1103 where K_{sat} is the saturated hydraulic conductivity; S_e is the saturation ratio and $S_e = (\theta - \theta_r) / (\theta_s - \theta_r)$;
1104 and L_e is the shape parameter ($L_e=0.5$; Mualem, 1976).

1105

1106 *Boundary conditions and surface energy balance*

1107 A zero-flow condition was assumed at the lower boundary of the peat column. The upper
1108 boundary condition was defined by the surface energy balance, which was driven by net
1109 radiation (Rn). The dynamics of Rn at surface x ($x=0$ for vascular canopy and $x=1$ for moss
1110 surface) was determined by the balance between incoming and outgoing radiation components:

$$1111 Rn_x = Rsn_{b,x} + Rsn_{d,x} + Rln_x \quad (A7)$$

1112 where $Rsn_{b,x}$ and $Rsn_{d,x}$ are the absorbed energy from direct and diffuse radiation; Rln_x is the
1113 absorbed net longwave radiation.

1114 Algorithms for calculating the net radiation components were detailed in Gong et al. (2013), as
1115 modified from the methods of Chen et al. (1999). Canopy light interception was determined by
1116 the light-extinction coefficient (k_{light}), leaf area index (Lc) and solar zenith angle. The
1117 partitioning of reflected and absorbed irradiances at ground surface was regulated by the surface
1118 albedos for the shortwave (a_s) and longwave (a_l) components, and the temperature of surface x
1119 (T_x) also affects net longwave radiation:

$$1120 Rn_x = Rsn_{b,x} + Rsn_{d,x} + Rln_x \quad (A8)$$

$$1121 Rsn_{d,x} = Rsid,x(1 - a_s) \quad (A9)$$

$$1122 Rln_x = Rli,x(1 - a_l) - \epsilon\delta T_x^4$$

1123 (A10)

1124 where Rsb , $Rsid$, Rli are the incoming beam, diffusive and longwave radiations; ϵ is the emissivity
1125 ($\epsilon = 1 - a_l$); δ is the Stefan Boltzmann's constant ($5.67 \times 10^{-8} \text{ W m}^{-2} \text{ K}^{-4}$).

1126 Rn_x was partitioned into latent heat flux (λE_x), sensible heat flux (H_x) and ground heat flux (for
1127 canopy $G_l=0$):

$$1128 Rn_x = H_x + \lambda E_x + G_x$$

1129 (A11)

$$1130 G_1 = K_T (T_x - Ts) / (0.5z) \quad (A12)$$

1131 where Ts is the temperature of the moss carpet; z is the thickness of the moss layer ($z = 5 \text{ cm}$).

1132 The latent heat flux was calculated by the “interactive scheme” (Daamen and McNaughton,
1133 2000; see also in Gong et al., 2016), which is a K-theory-based, multi-source model:

$$1134 \quad \lambda E_x = \frac{(\Delta/\gamma)A_x r_{sa,x} + \lambda VPD_b}{r_{b,x} + (\Delta/\gamma)r_{sa,x}} \quad (A13)$$

1135 where Δ is the slope of the saturated vapor pressure curve against air temperature; λ is the latent
 1136 heat of vaporization; E is the evaporation rate; VPD_b is the vapor pressure deficit at z_b ; $r_{b,x}$ is the
 1137 total resistance to water vapor flow, the sum of boundary layer resistance ($r_{sa,x}$) and surface
 1138 resistance (r_{ss}); and A is the available energy for evapotranspiration and $A_x = Rn_x - G_x$.

1139 The calculations of γ , λ and VPD_b require the temperature (T_b) and vapor pressure (e_b) at the
 1140 mean source height (z_b). These variables were related to the total of latent heat ($\sum \lambda E_x$) and
 1141 sensible heat ($\sum H_x$) from all surfaces using the Penman-type equations:

$$1142 \quad \sum \lambda E_x = \rho_a C_p (e_b - e_a) / (r_{aero} \gamma) \quad (A14)$$

$$1143 \quad \sum H_x = \rho_a C_p (T_b - T_a) / r_{aero} \quad (A15)$$

1145 where $\rho_a C_p$ is the volumetric specific heat of air; r_{aero} is the aerodynamic resistance between z_b
 1146 and the reference height z_a , and was a function of T_b accounting for the atmospheric stability
 1147 (Choudhury and Monteith, 1988); and γ is the psychrometric constant ($\gamma = \rho_a C_p / \lambda$).

1148 Changes in the energy balance affect the surface temperature (T_x) and vapor pressure (e_x), which
 1149 further feed back to the energy availability (Eq. A10, A12), the source-height temperature, VPD
 1150 and the resistance parameters (e.g., r_{aero}). The values of T_x and e_x were solved iteratively by
 1151 coupling the energy balance equations (eqs. A11–A15) with the Penman-type equations (see also
 1152 Appendix B in Gong et al., 2016):

$$1153 \quad \lambda E_x = \rho_a C_p (e_x - e_b) / (r_{sa,x} \gamma) \quad (A16)$$

$$1154 \quad H_x = \rho_a C_p (T_x - T_b) / r_{sa,x} \quad (A17)$$

1155 where the boundary-layer resistance for ground surface ($r_{sa,i}$) and canopy ($r_{sa,0}$) were calculated
 1156 following the approaches of Choudhury and Monteith (1988).

1157

1158 *Sink terms of transport functions for water and heat*

1159 The sink term $S_{h,i}$ (see Eq. A11) for each soil layer i was calculated as:

$$1160 \quad S_{h,i} = E_i - P_i - W_{melt,i} - I_i \quad (A18)$$

1161 where E_i is the evaporation loss of water from the layer; P_i is rainfall ($P_i = 0$ if the layer is not
 1162 topmost, i.e. $i > 1$); $W_{melt,i}$ is the amount of melt water added to the layer; I_i is the net water inflow
 1163 and was calibrated in Section 2.5.

1164 The value of E_i was calculated as:

165 $E_i = f_{top}E_0 + f_{root}(i)E_1$ (A19)

166 where E_0 and E_1 are the evaporation rate from ground surface and canopy (Eq. A13); f_{top} is the
 167 location multiplier for the topmost layer ($f_{top} = 0$ in cases $i > 1$); and $f_{root}(i)$ is the fraction of fine-
 168 root biomass in layer i .

169 The value of $W_{melt,i}$ was controlled by the freeze-thaw dynamics of soil water and snow pack,
 170 which were related to the heat diffusion in soil profile (Eq. A2). We set the freezing point
 171 temperature to 0 °C, and the temperature of a soil layer was held constant (0 °C) during freezing
 172 or melting. For the i th soil layer, the sink term (S_T) in heat transport equation (Eq. A2) was
 173 calculated as:

174 $S_{T,i} = f_{phase} \max(|T_i| C_{T,i}, W_{phase} \lambda_{melt})$ (A20)

175 where $C_{T,i}$ is specific heat of soil layer (Eq. A13); W_{phase} is the water content for freezing (W_{phase}
 176 = θ_w) or melting ($W_{phase} = \theta_{ice}$); λ_{melt} is the latent heat of freezing; f_{phase} is binarial coefficient that
 177 denotes the existence of freezing or thawing. For each time step t , we computed $T_i(t)$ with a piror
 178 assumption that $S_{T,i}=0$. Then f_{phase} was determined by whether the temperature changed across
 179 the freezing point, i.e. $f_{phase}=1$ if $T_i(t)*T_i(t-1) \leq 0$, otherwise $f_{phase}=0$.

180

181 Parameterization of SVAT processes

182 For the calculation of surface energy balance, we set the height and leaf area of vascular
 183 canopy to 0.4 m and 0.1 m² m⁻², consistent with the scarcity of vascular canopies at the site. The
 184 aerodynamic resistance (r_{aero} , Eq. A14, Appendix A) for surface energy fluxes was calculated
 185 following Gong et al. (2013a). The bulk surface resistance of community (r_{ss} , Eq. A13, Appendix
 186 A) was summarized from the cell-level values of $r_{bulk,i}$, that $1/r_{ss} = \sum(1/r_{bulk,i})$. To calculate the
 187 peat hydrology and water table, peat profiles of hummock and lawn communities were set to 150
 188 cm deep and stratified into horizontal layers of depths varying from 5cm (topmost) to 30cm
 189 (deepest). For each peat layer, the thermal conductivity (K_T) of fractional components, i.e. peat,
 190 water and ice, were evaluated following Gong et al. (2013a). The bulk density of peat (ρ_{bulk}) was
 191 set to 0.06 g cm⁻³ below acrotelm (40 cm depth, Laine et al., 2004), and decreased linearly
 192 toward the living moss layer. The saturated hydraulic conductivity (K_{sat} , Eq. A6, Appendix A)
 193 and water retention parameters (i.e. α and n , Eq. A5, Appendix A) of water retention curves were
 194 calculated as functions of ρ_{bulk} and the depth of peat layer following Päivänen (1973). K_{sat} , α and
 195 n for the living moss layer were adopted from the values measured by McCarter and Price (2014)
 196 from *S. magellanicum* carpet. The parameter values for SVAT processes are listed in Table 3.

197 Calculation of snow dynamics

198 In boreal and arctic regions, the amount and timing of snow melt has crucial impact on moisture

199 conditions, especially at fen peatlands. Therefore, to have realistic spring conditions we
200 introduced a snow-pack model, SURFEX v7.2 (Vionnet et al., 2007), into the SVAT modelling.
201 The snow-pack model simulates snow accumulation, wind drifting, compaction and changes in
202 metamorphism and density. These processes influenced the heat transport and freezing-melting
203 processes (i.e. S_h and S_T , see Eq. A1-A2, Appendix A). In this modelling, we calculate the snow
204 dynamics on a daily basis in parallel to the SVAT simulation. Daily snowfall was converted into
205 a snow layer and added to ground surface. For each of the day-based snow layers (D-layers), we
206 calculated the changes in snow density, particle morphology and layer thicknesses. At each time
207 step, D-layers were binned into layers of 5-10 cm depths (S-layers) and placed on top of the peat
208 column for SVAT modelling. With a snow layer present, surface albedos (i.e. a_s , a_l) were
209 modified to match those of the topmost snow layer (see Table 4 in Vionnet et al., 2007). If the
210 total thickness of snow was less than 5 cm, all D-layers were binned into one S-layer. The
211 thermal conductivity (K_T), specific heat (C_T), snow density, thickness and water content of each
212 S-layer were calculated as the mass-weighted means from the values of D-layers. Melting and
213 refreezing tended to increase the density and K_T of a snow layer but decrease its thickness (see
214 Eq. 18 in Vionnet et al., 2007). The fraction of melted water that exceeded the water holding
215 capacity of a D-layer (see Eq. 19 in Vionnet et al., 2007) was removed immediately as
216 infiltration water. If the peat layer underneath was saturated, the infiltration water was removed
217 from the system as lateral discharge.

218 *Boundary conditions and driving variables*

219 A zero-flow boundary was set at the bottom of peat. At peat surface the boundary conditions of
220 water and energy were defined by the ground surface temperature (T_0 , see Eq. A10-A15 in
221 Appendix A) and the net precipitation (P minus E). The profiles of layer thicknesses, ρ_{bulk} and
222 hydraulic parameters were assumed to be constant during simulation. Lateral boundary
223 conditions were used to calculate the spreading of *Sphagnum* shoots among cells along the edge
224 of the model domain so that shoots can spread across the edge of simulation area and invade into
225 the grid cell at the boarder of the opposite side.

226 The model simulation was driven by climatic variables of air temperature (T_a), precipitation
227 (P), relative humidity (R_h), wind speed (u), incoming shortwave radiation (R_s) and longwave
228 radiation (R_l). To support the stochastic parameterization of the model and Monte-Carlo
229 simulations, Weather Generator (Strandman et al., 1993) was used to generate randomized
230 scenarios based on long-term weather statistics (period of 1981-2010) from the four closest
231 weather stations of the Finnish Meteorological Institute. This generator had been intensively
232 tested and applied under Finnish conditions (Kellomäki and Väisänen, 1997; Venäläinen et al.,
233 2001; Alm et al., 2007). We also compared the simulated meteorological variables against 2-year
234 data measured from Siikaneva peatland site (61°50 N; 24°10 E), located 10 km away from our
235 study site (Appendix C).

1237 **Appendix B. Methods and results of the empirical study on *Sphagnum* capitula water**
1238 **retention as a controlling mechanism for peatland moss community dynamics**

1239

1240 *Measurement of morphological traits*

1241 To quantify morphological traits, samples of *S. fallax* and *S. magellanicum* were collected at the
1242 end of August 2016 with a core (size d 7cm, area 50 cm², height at least 8 cm) maintaining the
1243 natural density of the stand. Samples were stored in plastic bags at cool room (4 °C) until
1244 measurements. Eight replicates were collected for each species. For each sample, capitulum
1245 density (D_s , shoots cm⁻²) was measured and ten moss shoots were randomly selected and
1246 separated into capitula and stems (5 cm below capitula). The capitula and stems were moistened
1247 and placed on top of a tissue paper for 2 minutes to extract free-moving water, before weighing
1248 them for water-filled fresh weight. The samples were dried at 60 °C for at least 48h to measure
1249 the dry masses. The field-water contents of capitula (W_{cf} , g g⁻¹) and stems (W_{sf} , g g⁻¹) were then
1250 calculated as the ratio of water to dry mass for each sample. The biomass of capitula (B_{cap} , g m⁻²)
1251 and living stems (B_{st} , g m⁻²) were calculated by multiplying the dry masses with the capitulum
1252 density (D_s). Biomass density of living stems (H_{spc} , g cm⁻¹ m⁻²) was calculated by dividing B_{st}
1253 with the length of stems.

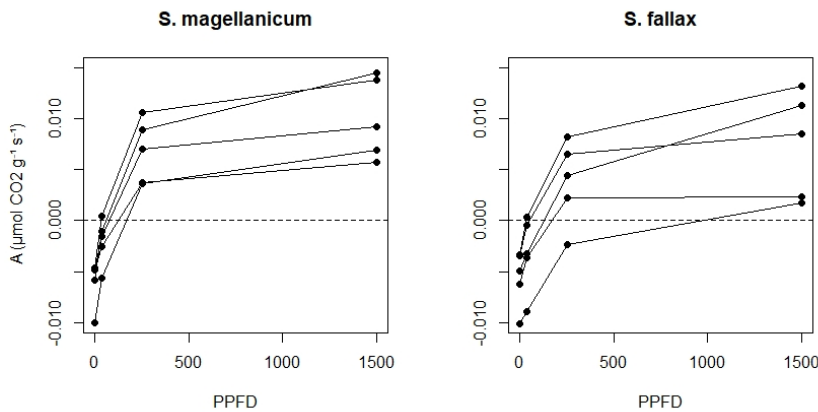
1254 *Measurement of photosynthetic traits*

1255 We measured the photosynthetic light response curves for *S. fallax* and *S. magellanicum* with
1256 fully controlled, flow-through gas-exchange fluorescence measurement systems (GFS-3000,
1257 Walz, Germany; Li-6400, Li-Cor, US) under varying light levels. In 2016, measurements on
1258 field-collected samples were done during May and early June, which is a peak growth period for
1259 *Sphagna* (Korrensalo et al. 2017). Samples were collected from the field site each morning and
1260 were measured the same day at Hyytiälä field station. Samples were stored in plastic containers
1261 and moistened with peatland water to avoid changes in plant status during the measurement.
1262 Right before the measurement we separated *Sphagnum* capitula from their stems and dried them
1263 lightly using tissue paper before placing an even layer of them in a custom-made cuvette by
1264 retaining the same density as naturally at field (Korrensalo et al. 2017). Net photosynthesis rate
1265 (A , $\mu\text{mol m}^{-2} \text{s}^{-1}$) was measured at 1500, 250, 35, and 0 $\mu\text{mol m}^{-2} \text{s}^{-1}$ photosynthetic photon
1266 flux density (PPFD) (Fig 1B). The light levels were chosen based on previous investigation by
1267 Laine et al. (2011, 2015), which showed increasing A until PPFD at 1500 and no photoinhibition
1268 even at high values of 2000 $\mu\text{mol m}^{-2} \text{s}^{-1}$. The samples were allowed to adjust to cuvette
1269 conditions before the first measurement and after each change in the PPFD level until the CO₂
1270 rate had reached a steady level, otherwise the cuvette conditions were kept constant (temperature
1271 20°C, CO₂ concentration 400 ppm, flow rate 500 $\mu\text{mol s}^{-1}$, impeller at level 5 and relative
1272 humidity of inflow air 60%, yet the relative humidity remained on average 81% during the
1273 measurements). The time required for a full measurement cycle varied between 60 and 120

1274 minutes. Each sample was weighed before and after the gas-exchange measurement, then dried
 1275 at 40°C for 48 h to determine the biomass of capitula (B_{cap}). For each species, ~~five~~ samples
 1276 were measured as replicates and were made to fit a hyperbolic light-saturation curve (Larcher,
 1277 2003):

$$1278 \quad A_{20} = \left(\frac{Pm_{20} * PPFD}{\alpha_{PPFD} + PPFD} - R_{S_{20}} \right) * B_{cap} \quad (B1)$$

1279 where subscript 20 denotes the variable value measured at 20 °C; R_s is the mass-based dark
 1280 respiration rate ($\mu\text{mol g}^{-1} \text{s}^{-1}$); Pm is the mass-based rate of maximal gross photosynthesis (μmol
 1281 $\text{g}^{-1} \text{s}^{-1}$); and α_{PPFD} is the half-saturation point ($\mu\text{mol m}^{-2} \text{s}^{-1}$), i.e., PPFD level where half of Pm is
 1282 reached. The measured morphological and photosynthetic traits are listed in Table 2.



1283
 1284 [Figure B1. Measured light response curves for *S. magellanicum* and *S. fallax*.](#)

1285
 1286 *Drying experiment*

1287 To link the water retention and photosynthesis of *Sphagnum* capitula, we performed a drying
 1288 experiment using a GFS-3000 system to measure co-variations of capitulum water potential (h ,
 1289 cm water), water content (W_{cap} , g g^{-1}) and A ($\mu\text{mol m}^{-2} \text{g}^{-1} \text{s}^{-1}$). For both species, four mesocosms
 1290 were collected in August 2018 and transported to laboratory in UEF Joensuu, Finland. Capitula
 1291 were harvested and wetted by water from the mesocosms. The capitula were then placed gently
 1292 on a piece of tissue paper for 2 minutes and then placed into the same cuvette as used in the
 1293 previous photosynthesis measurement. The cuvette was then placed into GFS and measured
 1294 under constant conditions of $PPFD$ ($1500 \mu\text{mol m}^{-2} \text{s}^{-1}$), temperature (293.2K), inflow air (700
 1295 $\mu\text{mol s}^{-1}$), CO_2 concentration (400 ppm) and relative humidity (40%). Measurement was stopped

1296 when A dropped to less than 10% of its maximum. Each measurement lasted between 120
 1297 and 180 minutes. Each sample was weighed before and after the gas-exchange measurement, then
 1298 dried at 40°C for 48 h to determine the biomass of capitula (B_{cap}).

1299 The GFS-3000 records the vapor pressure (e_a , kPa) and the evaporation rate (E , g s⁻¹)
 1300 simultaneously with A at every second (Heinz Walz GmbH, 2012). The changes in W_{cap} with
 1301 time (t) was calculated as following:

$$1302 \quad RWC(t) = (W_{pre} - B_c - \sum_{t=0}^t E(t)) / B_c \quad (B2)$$

1303 We assumed that the vapor pressure at the surface of water-filled cells equaled the saturation
 1304 vapor pressure (e_s), and the vapor pressure in the headspace of cuvette equaled that in the
 1305 outflow (e_a). The vapor pressure in capitula pores (e_i) thus can be calculated based on following
 1306 gradient-transport function (Fig. B2A):

$$1307 \quad \lambda E(t) = \frac{\rho_a c_p (e_i(t) - e_a(t))}{\gamma r_a(t)} = \frac{\rho_a c_p (e_s - e_i(t))}{\gamma r_s(t)} \quad (B3)$$

1308 where λ is the latent heat of vaporization; γ is the slope of the saturation vapor pressure -
 1309 temperature relationship; r_a is the aerodynamic resistance (m s⁻¹) for vapor transport from inter-
 1310 leaf volume to headspace; r_s is the surface resistance of vapor transport from wet leaf surface to
 1311 inter-leaf volume. The bulk resistance for evaporation (r_{bulk}) was thus calculated as $r_a + r_s$.

1312 We assumed that the structures of tissues and pores did not change during the drying process
 1313 and assumed r_a to be constant during each measurement. A tended to increase with time t until it
 1314 peaked (A_m) and then decreased (Fig. 2+B). The point $A=A_m$ implied the water content where
 1315 further evaporative loss would start to drain the cytoplasmic water, leading to the decrease in A .
 1316 The response of A to W_{cap} was fitted as a second-order polynomial function (Robroek et al.,
 1317 2009) using data from t_{Am} to t_n :

$$1318 \quad f_A(W_{cap}) = a_{w0} + a_{w1} * W_{cap} + a_{w2} * W_{cap}^2 \quad (B4)$$

1320 where a_{w0} , a_{w1} and a_{w2} are parameters; and $f_A(W_{cap}) = A/A_m$. For each replicate, the optimal water
 1321 content for photosynthesis (W_{opt}) was derived from the peak of fitted curve (Eq. 4). The
 1322 capitulum water content at the compensation point W_{cmp} , where the rates of gross photosynthesis
 1323 and respiration are equal, can be calculated from the point $A=0$.

1324
 1325
 1326
 1327

1328

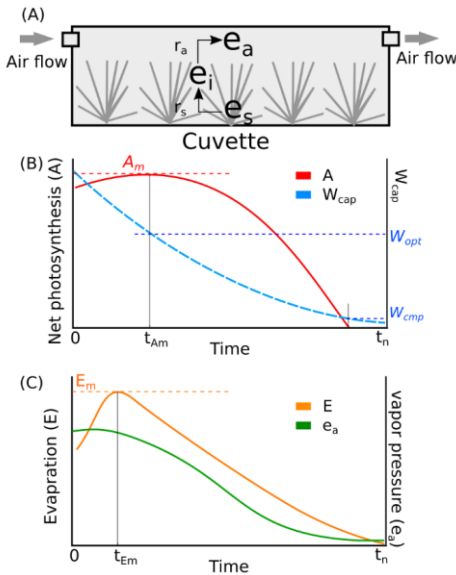


Figure B4.2. Conceptual schemes of (A) cuvette setting and resistances, (B) the co-variations of net photosynthesis and W_{cap} , and (C) the co-variations of evaporation and vapor pressure in headspace during a measurement. Meanings of symbols: e_a , vapor pressure in headspace of cuvette (kPa); e_i , vapor pressure in branch-leaf structure of capitula; e_s , vapor pressure at the surface of wet tissues; r_a , aerodynamic resistance of vapor diffusion from inner capitula to headspace; r_s , surface resistance of vapor diffusion from wet tissue surface to inner capitula space; A , net photosynthesis rate ($\mu\text{mol m}^{-2} \text{s}^{-1}$); A_m , maximal net photosynthesis rate ($\mu\text{mol m}^{-2} \text{s}^{-1}$); W_{cap} , water content of capitula (g g^{-1}); W_{opt} , W_{cap} at $A=A_m$; W_{cmp} , W_{cap} at $A=0$; E , evaporation rate (mm s^{-1}).

1346

1347

1348 Similarly, the evaporation rate (E) increased from the start of measurement until maximum
 1349 evaporation E_m , and then decreased (Fig. B4.2C). The point $E=E_m$ implied the time when the wet
 1350 capitulum tissues were maximally exposed to the air flow. Therefore, r_a was estimated as the
 1351 minimum of bulk resistance using Eq. (B5), by assuming $e_i(t) \approx e_s$ when $E(t) = E_m$:

$$1352 \quad r_a = \frac{\rho_a C_p (e_s - e_a(t))}{\gamma \lambda E_m} \quad (\text{B5})$$

1353 Based on the calculated $e_i(t)$, we were able to derive the capitulum water potential (h)
 1354 following the equilibrium vapor-pressure method (e.g. Price et al, 2008; Goetz and Price, 2015):

$$1355 \quad h = \frac{RT}{Mg} \ln \left(\frac{e_i}{e_s} \right) + h_0 \quad (\text{B6})$$

1356 where R is the universal gas constant ($8.314 \text{ J mol}^{-1} \text{ K}^{-1}$); M the molar mass of water (0.018 kg
 1357 mol^{-1}); g is the gravitational acceleration (9.8 N kg^{-1}); e_i/e_s is the relative humidity; h_0 is the
 1358 water potential due to the emptying of free-moving water before measurement (set to 10 kPa
 1359 according to Hayward and Clymo, 1982).

1360

1361 *Statistical analysis*

1362 The light response curve (Eq. B1) and the response function of A/A_m to W_{cap} changes (Eq. B4)
1363 were fitted using nlme package in R (version 3.1). The obtained values of shape parameters a_{w0} ,
1364 a_{w1} and a_{w2} (Eq. 4) were then used to calculate W_{opt} ($W_{opt} = -0.5 a_{w1} / a_{w2}$) and W_{cmp} ($W_{cmp} = 0.5$
1365 $[-a_{w1} - (a_{w1}^2 - 4a_{w0} a_{w2})^{0.5}] / a_{w2}$). We then applied ANOVA to compare *S. magellanicum* against
1366 *S. fallax* for the traits obtained from the field sampling (i.e. structural properties such as B_{cap} , D_S ,
1367 H_{spc} , W_{cf} , W_{sf}) and from the gas-exchange measurements (i.e. Pm_{20} , Rs_{20} , W_{opt} , W_{cmp} and r_{bulk}),
1368 using R (version 3.1).

1369 The measured values of capitulum water potential (h) were \log_{10} -transformed and related to the
1370 variations in W_{cap} , B_{cap} and D_S with a linear model. Similarly, a linear model was established to
1371 quantify the response of bulk resistance for evaporation (r_{bulk}) (\log_{10} -transformed) to the
1372 variations in h , B_{cap} and D_S . The linear regressions were based on statsmodels (version 0.9.0) in
1373 Python (version 2.7), as supported by Numpy (version 1.12.0) and Pandas (version 0.23.4)
1374 packages.

1375

1376 **Results of the empirical measurements**

1377 The two *Sphagnum* species differed in their structural properties (Table B1). Lawn species *S.*
1378 *fallax* had looser structure than hummock species *S. magellanicum* as seen in lower capitulum
1379 density (D_S) and specific height (H_{spc}) in *S. fallax* than in *S. magellanicum* ($P < 0.05$, Table. B1).
1380 Moreover, in conditions prevailing in the study site *S. fallax* mosses were dryer than *S.*
1381 *magellanicum*; the field-water contents of *S. fallax* capitulum (W_{cf}) and stem (W_{sf}) were 40% and
1382 46% lower than *S. magellanicum* ($P < 0.01$, Table. B1), respectively. The different density of
1383 capitulum of the two species differing in their capitulum size led to similar capitulum biomass
1384 (B_{cap}) ($P = 0.682$) between *S. fallax* with small capitulum and *S. magellanicum* with large
1385 capitulum. Unlike the structural properties, maximal CO_2 exchange rates (Pm_{20} and Rs_{20}) did not
1386 differ between the two species (Table B1).

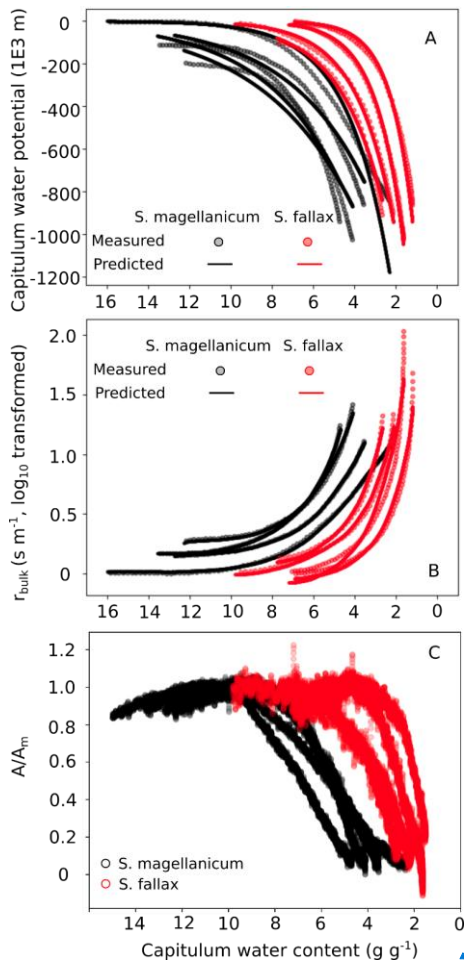
1387 The drying experiment demonstrated how capitulum water content regulated capitulum
1388 processes in both studied *Sphagnum* species (Fig. B23). Decreasing capitulum water content
1389 (W_{cap}) led to decrease in the water potential (h), the responses of h to W_{cap} varied among
1390 replicates (Fig. 23A). The values of W_{cap} for *S. fallax* were generally lower than those for *S.*
1391 *magellanicum* under the same water potentials. The fitted linear models explained over 95% of
1392 the variations in the measured h for both species (Table. B2), although fitted responses of h to
1393 W_{cap} were slightly smoother than the measured ones, particularly for *S. magellanicum* (Fig.
1394 B23A). The responses of h to W_{cap} was significantly affected by the capitulum density (D_S),
1395 capitulum biomass (B_{cap}) and their interactions with W_{cap} (Table. B2).

1396 Decreasing capitulum water content (W_{cap}), and water potential (h), were associated with

1397 increasing bulk resistance for evaporation (r_{bulk} , Fig. B23B), although the sensitivity of r_{bulk} to h
1398 changes varied by replicates. The values of r_{bulk} from *S. fallax* were largely lower than those
1399 from *S. magellanicum* when the capitulum water content of the two species were similar. The
1400 fitted linear models explained the observed variations in the measured r_{bulk} well for both species
1401 (Fig. 2B and Table. B3). The variation in the response of r_{bulk} to h was significantly affected by
1402 capitulum density (D_S), capitulum biomass (B_{cap}) and their interactions with h (Table. B3).

1403 Decreasing capitulum water content (W_{cap}) slowed down the net photosynthesis rate (Fig.
1404 B2C), as represented by the decreasing ratio of A/A_m . *S. fallax* required lower capitulum water
1405 content (W_{cap}) than *S. magellanicum* to reach photosynthetic maximum and photosynthetic
1406 compensation point. However, the ranges of capitulum water content from photosynthetic
1407 maximum (W_{opt}) or field capacity (W_{fc}) to that at compensation point (W_{cmp}) were smaller for *S.*
1408 *fallax* than *S. magellanicum*. Hence, *S. fallax* had narrower transition zone for photosynthesis to
1409 respond to drying, compared to *S. magellanicum*.

1410
1411



412

413 Figure B23. Responses of (A) capitulum water potential, (B) bulk resistance of evaporation, and
 414 (C) net photosynthesis to changes in capitulum water content (W_{cap}) of two *Sphagnum* species
 415 typical to hummocks (*S. magellanicum*, black) and lawns (*S. fallax*, red). As the measured results
 416 are based on the drying experiment starting with fully wetted capitula characteristic for both
 417 species, the X-axis is shown from high to low W_{cap} . The values predicted in (B) and (C) are
 418 based on linear models with parameter values listed in Tables B2 and B3 and predictor values
 419 from the drying experiment.

420

421

422

423
424
425
426
427

Table. B1 Species-specific traits of morphological, photosynthetic and water-retention from *S. magellanicum* and *S. fallax*. Trait values (mean \pm standard deviation) and ANOVA statistics F- and p-values are given for comparing the means of traits of the two species.

Trait	<i>S. magellanicum</i>	<i>S. fallax</i>	F	P (>F)
Capitulum density, D_S (capitula cm^{-2})	0.922 \pm 0.289	1.46 \pm 0.323	6.224 ^a	0.037 *
Capitulum biomass, B_{cap} (g m^{-2})	75.4 \pm 21.5	69.2 \pm 19.6	0.181 ^a	0.682
Specific height, H_{spc} ($\text{cm g}^{-1} \text{m}^{-2}$)	45.4 \pm 7.64	32.6 \pm 6.97	6.126 ^a	0.038*
Field water content of capitula, W_{cf} (g g^{-1})	14.7 \pm 3.54	8.09 \pm 1.48	11.75 ^a	0.009**
Field water content of stems, W_{sf} (g g^{-1})	18.4 \pm 1.92	10.2 \pm 1.50	45.81 ^a	0.0001**
Maximal gross photosynthesis rate at 20 °C, Pm_{20} ($\mu\text{mol g}^{-1} \text{s}^{-1}$)	0.019 \pm 0.004	0.014 \pm 0.002	3.737 ^b	0.101
Respiration rate at 20 °C, Rs_{20} ($\mu\text{mol g}^{-1} \text{s}^{-1}$)	0.007 \pm 0.004	0.007 \pm 0.002	0.012 ^b	0.92
half-saturation point of photosynthesis, α_{PPFD} ($\mu\text{mol g}^{-1} \text{s}^{-1}$)	101.4 \pm 14.1	143 \pm 51.2	2.856 ^b	0.142
Optimal capitulum water content for photosynthesis, W_{opt} (g g^{-1})	9.41 \pm 0.73	5.81 \pm 1.68	11.57 ^b	0.0145*
Capitulum water content at photosynthetic compensation point, W_{cmp} (g g^{-1})	3.67 \pm 0.83	1.78 \pm 0.43	12.35 ^b	0.0126*
Minimal bulk resistance of evaporation, r_a (m s^{-1})	33.5 \pm 7.30	40.7 \pm 4.99	1.976 ^b	0.2165

428 ^a soil-core measurement, sample $n=5$; ^b cuvette gas-exchange measurement, sample $n=4$; * the
429 difference of means is significant ($P<0.05$); ** the difference of means is very significant
430 ($P<0.01$).

431
432

433 Table B2. Parameter estimates of the linear model for the log₁₀-transformed capitulum water
 434 potential (*h*) for *S. fallax* and *S. magellanicum*. Estimate value, standard error (SE), and test
 435 statistics p-values are given to the predictors of the models. Predictors are: capitulum biomass
 436 (B_{cap}), capitulum density (D_S), capitulum water content (W_{cap}), the interaction of capitulum
 437 biomass and water potential ($B_{cap} \times W_{cap}$), the interactions of capitulum biomass and capitulum
 438 density ($D_S \times W_{cap}$), the interactions of capitulum density and water potential ($D_S \times W_{cap}$), and the
 439 interaction of capitulum biomass, capitulum density and water potential ($B_{cap} \times D_S \times W_{cap}$). All
 440 coefficient values are significantly different from 0 ($p < 0.001$).

Parameter	<i>S. magellanicum</i> ($R^2=0.972$)		<i>S. fallax</i> ($R^2=0.984$)	
	Value	SE	Value	SE
(Intercept)	25.30	0.253	-90.99	2.158
B_{cap}	-272.10	3.133	2294.67	52.342
W_{cap}	-9.50	0.031	-62.12	0.600
$B_{cap} \times W_{cap}$	114.61	0.387	1500.26	14.549
D_S	-21.76	0.253	104.11	2.376
$B_{cap} \times D_S$	268.95	3.112	-2422.79	55.251
$D_S \times W_{cap}$	9.33	0.031	68.35	0.661
$B_{cap} \times D_S \times W_{cap}$	-113.33	0.386	-1588.06	15.360

441

442

443

1444

1445 Table B3. Parameter estimates of the linear model for the \log_{10} -transformed capitulum
 1446 evaporative resistance (r_{bulk}) for *S. fallax* and *S. magellanicum*. Estimate value, standard error
 1447 (SE), and test statistics p-values are given to the predictors of the models. Predictors are:
 1448 capitulum biomass (B_{cap}), capitulum density (D_S), water potential (h), the interaction of
 1449 capitulum biomass and water potential ($B_{cap} \times h$), the interactions of capitulum biomass and
 1450 capitulum density ($D_S \times h$), the interactions of capitulum density and water potential ($D_S \times h$), and
 1451 the interaction of capitulum biomass, capitulum density and water potential ($B_{cap} \times D_S \times h$). All
 1452 coefficient values are significantly different from 0 ($p < 0.001$).

Parameter	<i>S. magellanicum</i> ($R^2=0.998$)		<i>S. fallax</i> ($R^2=0.966$)	
	Value	SE	Value	SE
(Intercept)	-1.13	0.027	55.07	2.225
B_{cap}	14.45	0.334	1334.55	53.968
h	0.0012	5.92e-05	-0.028	0.004
$B_{cap} \times h$	-0.0007	0.001	0.707	0.101
D_S	1.08	0.027	-60.53	2.450
$B_{cap} \times D_S$	-13.39	0.333	1406.36	56.968
$D_S \times h$	0.0002	5.89e-05	0.0317	0.005
$B_{cap} \times D_S \times h$	-0.0017	0.001	-0.733	0.106

1453

1454

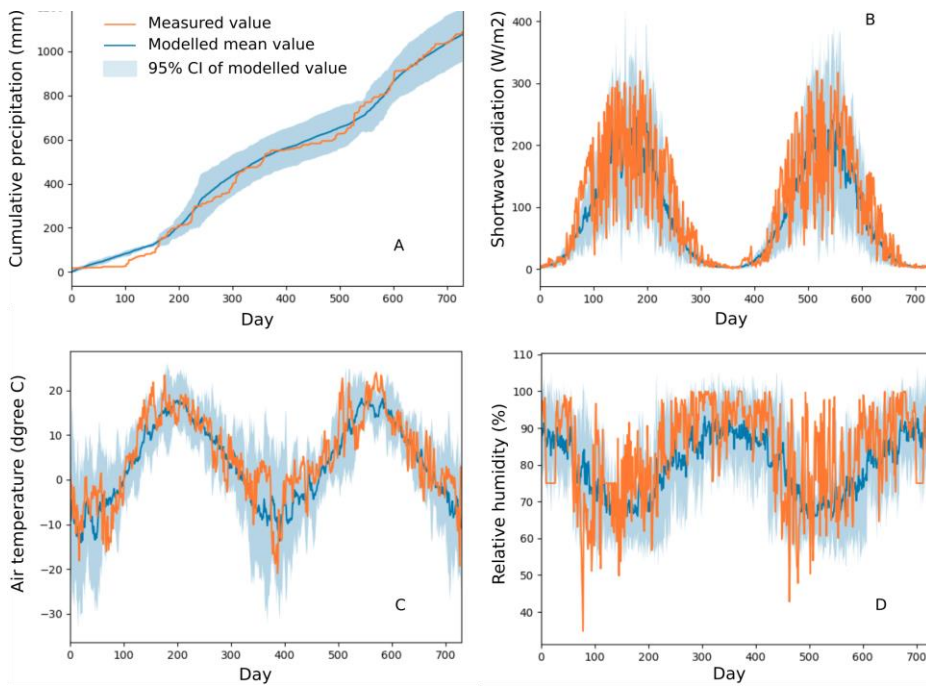
References

- 1456 Goetz, J. D. and Price, J. S.: Role of morphological structure and layering of *Sphagnum* and
 1457 *Tomenthypnum* mosses on moss productivity and evaporation rates, Canadian Journal of Soil
 1458 Science, 95, 109-124, 2015.
- 1459 Hayward P. M. and Clymo R. S.: Profiles of water content and pore size in Sphagnum and peat,
 1460 and their relation to peat bog ecology. Proceedings of the Royal Society of London, Series B,
 1461 Biological Sciences, 215, 299-325, 1982.
- 1462 Korrensalo, A., Alekseychik, P., Hájek, T., Rinne, J., Vesala, T., Mehtätalo, L., Mammarella, I.
 1463 and Tuittila, E.-S.: Species-specific temporal variation in photosynthesis as a moderator of
 1464 peatland carbon sequestration, Biogeosciences, 14, 257-269, 2017.
- 1465 Laine, A. M., Juurola, E., Hájek, T., & Tuittila, E. S.: Sphagnum growth and ecophysiology
 1466 during mire succession. Oecologia, 167(4), 1115-1125, 2011.
- 1467 Laine, A. M., Ehonen, S., Juurola, E., Mehtätalo, L., & Tuittila, E. S.: Performance of late
 1468 succession species along a chronosequence: Environment does not exclude *Sphagnum fuscum*

- 1469 from the early stages of mire development. *Journal of vegetation science*, 26(2), 291-301, 2015.
- 1470 Larcher, W.: *Physiological Plant Ecology: Ecophysiology and Stress Physiology of Functional*
1471 *Groups*, Springer, 2003.
- 1472 Price, J. S., Whittington, P. N., Elrick, D. E., Strack, M., Brunet, N. and Faux, E.: A method to
1473 determine unsaturated hydraulic conductivity in living and undecomposed moss, *Soil Sci. Soc.*
1474 *Am. J.*, 72, 487 – 491, 2008.
- 1475 Robroek, B. J.M., Schouten, M. G.C., Limpens, J., Berendse, F. and Poorter, H.: Interactive
1476 effects of water table and precipitation on net CO₂ assimilation of three co-occurring *Sphagnum*
1477 mosses differing in distribution above the water table, *Global Change Biology* 15, 680 – 691,
1478 2009.

1479 **Appendix C. Comparisons of meteorological variables simulated by Weather Generator**
1480 **and those measured from Siikaneva peatland site (ICOS site located in 10 km distance**
1481 **from the study site Lakkasuo)**

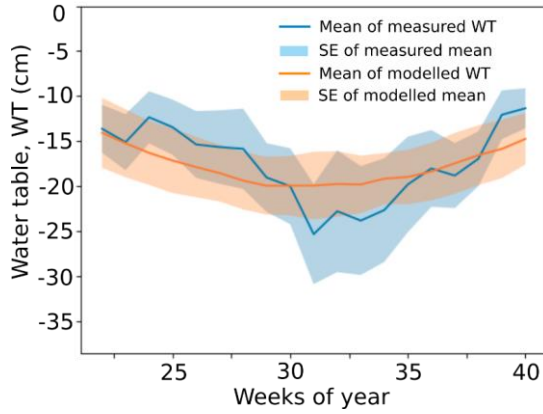
1482



1483 Fig. C1 Comparisons of meteorological variables simulated by Weather Generator and those
1484 measured from Siikaneva peatland site. The variables include (A) cumulative precipitation (mm),
1485 (B) incoming shortwave radiation ($W m^{-2}$), (C) air temperature ($^{\circ}C$), and (D) relative humidity
1486 (%). These variables were measured and simulated at half-hourly timescale. The measurements
1487 were carried out during 2012-2013. Details about the site and measurements have been described
1488 by Alekseychik et al. (2018). The measured seasonal dynamics of the meteorological variables
1489 were generally in line with the 95% confidence intervals (CI) of the simulated values, which
1490 were calculated based on Monte-Carlo simulations ($n=5$).

1491

1492 **Appendix D. Comparisons of seasonal water table measured from the study site and the**
1493 **values simulated based on calibrated net inflow**



1494

1495 Fig. D1 Comparison of seasonal water table (WT) measured at the Lakkasuo study site and the
1496 values simulated by the calibrated PCS. WT values were sampled weekly from the lawn habitats
1497 both in field and in model output. The weekly mean WT was measured during 2001, 2002, 2004
1498 and 2016. The modelled means and standard deviations (SD) of WT were based on 20 Monte-
1499 Carlo simulations. The simulated seasonality of mean WT generally followed the measured
1500 trends. The calibration reduced the sum of squared error (SE, Eq. 12) from 199.5 ($a_N=b_N=0$) to
1501 117.3. The calibrated values for a_N and b_N were $-5.3575 \cdot 10^{-4}$ and $4.7599 \cdot 10^{-5}$, respectively (Eq.
1502 A18).